DOI: 10.1534/genetics.105.043125

Identification of Genetic Loci That Interact With *cut* During Drosophila Wing-Margin Development

Joshua J. Krupp,*,† Lauren E. Yaich,‡ Robert J. Wessells* and Rolf Bodmer*,[1]

**The Burnham Institute, La Jolla, California 92037,* †*Neuroscience Program, University of Michigan, Ann Arbor, Michigan 48109 and* ‡*Biological and Health Sciences Division, University of Pittsburgh, Bradford, Pennsylvania 16701*

Manuscript received March 10, 2005
Accepted for publication May 11, 2005

ABSTRACT

The Drosophila selector gene *cut* is a hierarchal regulator of external sensory organ identity and is required to pattern the sensory and nonsensory cells of the wing margin. Cut performs the latter function, in part, by maintaining expression of the secreted morphogen encoded by *wingless* (*wg*). We find that Cut is required for wing-margin sensory organ specification in addition to and independently of Wg maintenance. In addition, we performed a genetic modifier screen to identify other genes that interact with *cut* in the regulation of wing-margin patterning. In total, 45 genetic loci (35 gain-of-function and 10 loss-of-function loci) were identified by virtue of their ability to suppress the wing-margin defects resulting from gypsy retrotransposon-mediated insulation of the *cut* wing-margin enhancer. Further genetic characterization identified several subgroups of candidate *cut* interacting loci. One group consists of putative regulators of gypsy insulator activity. A second group is potentially required for the regulation of Cut expression and/or activity and includes *longitudinals lacking*, a gene that encodes a family of BTB-domain zinc-finger transcription factors. A third group, which includes a component of the Brahma chromatin remodeling complex encoded by *moira*, affects the level of Cut expression in two opposing ways by suppressing the gypsy-mediated ct^{K} phenotype and enhancing the non-gypsy ct^{53d} phenotype. This suggests that the Brahma complex modulates both enhancer-controlled transcription and gypsy-mediated gene insulation of the *cut* locus.

SELECTOR genes are hierarchal regulators of developmental programs controlling tissue and cell-type diversification. The highly conserved Hox class of homeotic selector genes, which control the specification of regional identity along the anterior/posterior axis, exemplifies the ability of selector genes to instructively direct the selection between alternative developmental states. For instance, gain-of-function mutations in the Hox gene *Antennapedia* (*Antp*), resulting in the inappropriate expression of Antp protein in imaginal antennal tissue, lead to complete antenna-to-leg transformations (Schneuwly *et al.* 1987). It has been proposed that selector genes function by coordinating the serial activity of "realizator" genes (*i.e.*, those genes that intimately affect basic cellular processes directing cell growth, shape, migration, proliferation, and death, among others; Garcia-Bellido 1975). Identified realizator genes include β*3-tubulin* (Kremser *et al.* 1999) and *centrosomin* (Heuer *et al.* 1995), both of which affect cyto-architectural organization, the cell adhesion molecule encoded by *Connectin* (Gould and White 1992), and the pro-apoptotic gene *reaper* (Lohmann *et al.* 2002). In addition to the immediate regulation of realizator gene activity, selector genes also control and integrate intermediary transcriptional and cell-signaling networks that indirectly link selector gene activity with realizator functions (reviewed in Mann and Carroll 2002; Hombria and Lovegrove 2003). Thus, to understand how selector genes define alternative developmental states, it is necessary to identify the downstream regulatory networks, as well as the realizator genes, which ultimately carry out the selected developmental program.

The *Drosophila melanogaster* gene *cut* is a neural selector gene, which establishes the developmental program directing external sensory (ES) organ identity. The peripheral nervous system is composed of diverse types of sensory organs, including ES organs (cuticular mechanosensory and chemosensory sensilla) and chordotonal organs (subcuticular proprioceptive organs). Although morphologically dissimilar, these sensory organs share molecular and developmental similarities suggestive of a common evolutionary origin (reviewed in Lai and Orgogozo 2004). During embryonic and pupal development Cut is specifically expressed in the neuroepithelial-derived sensory organ precursor cells (SOP cells) from which emerge the lineage-related cells of individual ES organs (Blochlinger *et al.* 1990). Loss of *cut* function results in the morphological and molecular transformation of ES organs into chordotonal organs (Bodmer *et al.* 1987; Merritt 1997). Conversely, the ubiquitous misexpression of Cut transforms chordoto-

[1]*Corresponding author:* The Burnham Institute, 10901 N. Torrey Pines Rd., La Jolla, CA 92037. E-mail: rolf@burnham.org

nal organs into ES organs (Blochlinger *et al.* 1991). The overexpression of Cut directs ES organ identity only in cells predetermined with proneural character (*i.e.*, ES and chordotonal organ SOP cells) and acts in concert with factors common to these early precursor cells to direct ES organ identity. Thus *cut* represents a neural selector gene, the presence or absence of which is sufficient to direct alternative sensory organ fates. It is not known what downstream targets or realizator genes Cut regulates to instruct ES organ identity. The only putative Cut transcriptional target implicated in sensory organ specification is the gene *bereft* (*bft*), which is required for bristle morphogenesis (Hardiman *et al.* 2002).

cut is involved in the development of several embryonic and adult tissues, including the Malpighian tubules (Liu *et al.* 1991; Liu and Jack 1992), posterior spiracles (Hu and Castelli-Gair 1999), egg chamber (Jackson and Blochlinger 1997; Jackson and Berg 1999), flight muscles (Sudarsan *et al.* 2001), and wing margin (Micchelli *et al.* 1997). Additionally, the level of Cut expression regulates the degree of dendritic branching in a subset of multiple dendritic neurons (Grueber *et al.* 2003). It is not clear if *cut* acts as a selector gene in the development of these tissues (Liu and Jack 1992; Hu and Castelli-Gair 1999). In the developing wing, *cut* is required for proper patterning of the wing margin via complex interactions with multiple signaling pathways, including the Wingless (Wg) and Notch pathways (Micchelli *et al.* 1997). The absence of Cut activity leads to the nonautonomous degeneration of wing tissue, producing the classical "cut" wing phenotype (Jack *et al.* 1991). Degeneration of margin cells prefigures the development of several rows of ES organs arrayed along the anterior wing margin. It is conceivable that Cut is required early to convey a survival signal, most likely via the maintenance of Wg expression (Johnston and Sanders 2003), in addition to a later role in the specification of margin ES organ identity.

cut encodes a highly conserved homeodomain transcription factor with three novel DNA-binding domains, termed CUT repeats (Blochlinger *et al.* 1988; Andres *et al.* 1994; Moon *et al.* 2000). Vertebrate *cut* homologs, including mouse *Cux1* and *Cux2* (Valarche *et al.* 1993; Quaggin *et al.* 1996; Zimmer *et al.* 2004) and human *CDP* (Neufeld *et al.* 1992), are postulated to regulate cell growth and terminal differentiation. In diverse systems, Cut homologs functionally interact with the regulatory regions of developmentally active genes, including human *histone H4* (van Wijnen *et al.* 1996; Gupta *et al.* 2003), *lactoferrin* (Khanna-Gupta *et al.* 1997, 2003), *myeloid cytochrome heavy chain* (*gp91-phox*; Skalnik *et al.* 1991; Lievens *et al.* 1995), and *DNA polymerase* α (Truscott *et al.* 2003), as well as mouse *N-CAM* (Valarche *et al.* 1993) and *immunoglobulin heavy chain* (*IgH*) (Wang *et al.* 1999), among others. The targeted disruption of murine *Cux1* disrupts normal growth control and dermal tissue development (Ellis *et al.* 2001; Sinclair *et al.* 2001; Luong *et al.* 2002). Constitutive overexpression of Cux1 results in multiple organ hyperplasia, a phenotype partially attributable to the downregulation of the cyclin kinase inhibitor $p27^{kip1}$ (Ledford *et al.* 2002). Consistent with these results, the DNA-binding ability of CDP/Cux1 is post-translationally regulated in a cell-cycle-dependent manner (Coqueret *et al.* 1998; Moon *et al.* 2001; Santaguida *et al.* 2001; Goulet *et al.* 2004), suggesting that CDP/Cux1 may act as part of a transcriptional network controlling the G_1/S phase transition. Less is known about the function of murine *Cux2*. However, the dynamic expression pattern of *Cux2* mRNA in the central nervous system, particularly in the subventricular zone and upper cortical layers of the developing telencephalon, suggests that *Cux2* regulates a pool of cycling precursor cells predetermined to generate upper-layer cortical neurons (Zimmer *et al.* 2004). Interestingly, murine Cux1 and human CDP have been shown to functionally substitute for Drosophila Cut during embryonic development (Ludlow *et al.* 1996; Grueber *et al.* 2003), signifying a high degree of structural and functional conservation. It is not clear, however, if mammalian *CDP/Cux1* genes act as selector genes in their native developmental context.

To identify genes that interact with Drosophila *cut*, we conducted complementary gain-of-function and loss-of-function genetic suppressor screens. For this purpose, we created >2000 new Drosophila lines, each carrying a unique insertion of the modular UAS/GAL4-based Gene Search (GS) vector (Toba *et al.* 1999). The GS vector contains bidirectional upstream activating sequences (UAS), which bind the transcriptional activator Gal4. Under the control of wing-margin-specific Gal4 expression, genes located near the GS vector insertion site were misexpressed and scored according to their ability to suppress the adult *cut* wing phenotype. Additionally, 158 deficiency chromosomes (second and third chromosomes) covering ~50% of the genome were tested for the ability to dominantly suppress the *cut* allele ct^K. Of the genes that were identified through these screens, the BTB-domain zinc-finger gene *longitudinals lacking* (*lola*) and several genes encoding subunits of the Brahma chromatin-remodeling complexes were investigated further with regard to their interaction with *cut* during wing-margin development. The genetic interactions between these genes and *cut* suggest that they are involved in modulating the level of Cut expression and thus act together with Cut to pattern wing-margin tissues.

MATERIALS AND METHODS

Drosophila strains and culture: *D. melanogaster* stocks were reared on standard cornmeal/molasses media at room temperature or at 18°. Crosses were initiated and maintained at 25°. The *cm, ct^{53d}*, and *yw^{67c23}, ct^{2s}* lines were provided by D. Dorsett. The amorphic *$lola^{5D2}$*, *$lola^{ORE76}$*, and *$lola^{ORE120}$* alleles and the decision-

selective *lola*^{ORC4} and *lola*^{ORE119} alleles were provided by E. Giniger and are described elsewhere (Goeke *et al.* 2003). Transgenic *UAS-Brm*^{K804R}, *UAS-osa*^{s2}, *UAS-Osa*$^{RD[11c]}$, and *UAS-Osa*$^{AD[20e]}$ lines were provided by J. Treisman and are described elsewhere (Elfring *et al.* 1998; Collins *et al.* 1999). The *GS-V[1]* stock was a generous gift from T. Aigaki (Toba *et al.* 1999). The *ct*^{K}, *ct*^{6}, *mor*^{1}, *brm*^{2}, *snr1[01319], UAS-wg, UAS-p35*, and all deficiency lines were obtained from the Bloomington Stock Center. The *ct*^{53d} and *ct*^{2s} stocks carry overlapping deletions of ~500 bp and 1.6 kb, respectively, of the *cut* wing-margin enhancer, which is positioned ~−80 kb upstream of the first exon (Liu *et al.* 1991; Mogila *et al.* 1992). The *ct*^{K} and *ct*^{6} alleles result from insertions of the gypsy retrotransposon between the wing enhancer and the first exon. The *ct*^{K} insertion is located −6 kb upstream of the 5′-most exon (Liu *et al.* 1991), whereas the *ct*^{6} insertion is located proximal to the wing enhancer (Dorsett 1993). Descriptions of the other gene mutations and deficiency chromosomes can be found on FlyBase (http://flybase.boi.indiana.edu).

The *C96-Gal4* driver line carries a *P{GawB}* insertion at the 70D locus near the *C96* gene; a gene required for viability and imaginal disc development (Gustafson and Boulianne 1996; Kim and Boulianne 1998). Flies homozygous for the *P{GawB}C96* insertion are homozygous viable and wing development is normal. The *P{GawB}C96* insertion directs Gal4 expression in a broad stripe straddling the dorsoventral boundary of the wing imaginal disc, which corresponds to the anlage of the adult wing margin and the cells expressing Cut. *P{GawB}C96*-driven Gal4 expression is unaffected by hypomorphic *cut* mutations.

Deficiency screen: Prior to initiating the deficiency screen, the *ct*^{K} stock was isogenized for the second and third chromosomes by first crossing females from a wild-type Oregon-R stock to males from the double balancer stock *ct*^{K}*/Y*; *Pin/CyO*; *D/TM6B*. Individual F_1 +/*ct*^{K}; +/*CyO*; +/*TM6B* females were backcrossed to *ct*^{K}; *Pin/CyO*; *D/TM6B* males. Stable isogenic *ct*^{K}; +/+; +/+ stocks were maintained by crossing balanced F_2 *ct*^{K}; +/*CyO*; +/*TM6B* siblings derived from individual F_1 females. The *ct*^{K} stock was again isogenized after the initial screen and interacting deficiencies were rechecked. The use of two different isogenic stocks controlled for any phenotypes caused by differences in genetic background. To test for genetic interactions, female flies homozygous for *ct*^{K} were crossed to male flies containing the deficiency chromosome (Df) over a marked balancer. The wings of male progeny that were *ct*^{K}*/Y*; *Df/+* were examined for a decrease in the penetrance of the *ct*^{K} phenotype (see below).

Generation and screening of GS vector insertion lines: The GS vector as described by Toba *et al.* (1999) contains two copies of the sequence UAS (originating form *Saccharomyces cerevisiae*) adjacent to a core promoter. UAS/core promoter sites are proximal to the terminal inverted repeat sequences located at either end of the *P*-element vector and oriented as to mediate transcription outward in both directions. Independent GS vector insertion lines were generated by mobilizing the GS vector, located on a *CyO* chromosome, with Δ*2-3* transposase (Robertson *et al.* 1988). The reinsertion of the mobilized GS vector was identified via the expression of the *mini-white* gene. Independent reinsertion events in the second and third chromosomes were balanced with *SM5-TM6*, a reciprocal translocation balancer. Stable stocks were maintained over the *SM5-TM6* balancer or, if possible, in a homozygous state.

To identify genetic loci that suppress the *ct*^{K} wing phenotype, three male flies from each of 2066 individual GS lines, with insertions on the second or third chromosomes, were crossed to six females of the genotype *w,ct*$^{K;C96\text{-}Gal4}$. The penetrance of the *cut* wing phenotype of male progeny of the genotype *ct*^{K}*/Y;GS*/C96-Gal4* was compared to *ct*^{K}*/Y;C96-Gal4/UAS-lacZ* and *ct*^{K}*/Y;C96-Gal4/+* controls. The controls showed a completely penetrant (>99%) *ct*^{K} wing phenotype, as demonstrated by numerous discontinuities (*i.e.*, gaps) in the regular array of wing-margin sensory bristles and frequent incisions of wing tissue. The expressivity of the *ct*^{K} wing phenotype was identical for both controls. In the initial testing of all 2066 GS lines and the 158 deficiencies, 20–40 males of the genotypes *ct*^{K}*;GS*/C96-Gal4* or *ct*^{K}*;Df/+* were examined. In addition, females were examined for dominant effects. Due to the prevalence of dominant effects that enhanced the *ct*^{K} phenotype resulting from the overexpression of the various GS insertions, we opted not to characterize these lines further. Those lines (GS or deficiency) that were found to suppress the *ct*^{K} phenotype were retested. GS lines were retested by crossing to both *ct*^{K}*; C96-Gal4* and *ct*^{K} alone to determine if suppression resulted from overexpression or from gene disruption. In all cases, >100 *ct*^{K} males were screened in the retests. Identical but independent crosses produced similar results in the majority of cases. To confirm the interaction with *cut*, GS lines were secondarily tested for the ability to interact with *ct*^{53d}*; C96-Gal4*. The presence of discontinuities in the anterior wing margin of *ct*^{53d}*/Y;C96-Gal4/UAS-lacZ* and *ct*^{53d}*/Y;C96-Gal4/+* controls were less penetrant (~50–60%) than with *ct*^{K}, allowing increases (enhancement) or decreases (suppression) in penetrance to be scored. To maintain consistency, all crosses were performed with *cut* alleles in the presence of the *P{GawB}C96* insertion. The presence of *P{GawB}C96* did not influence the interaction between any of the loss-of-function mutations and *cut*.

Individual GS insertion lines were scored according to their ability to suppress or enhance the penetrance of the *cut* wing phenotype. For our purposes, only a discrete region of the anterior wing margin, consisting of the region stretching from the proximal-most point of the anterior wing margin to the distally located intersection of the L1 and L2 wing veins (see Figure 1C), was scored. This region was chosen because it encompasses most of the triple row of innervated sensory bristles and can be easily examined in anesthetized intact animals with their wings tucked back in the resting position. In cases in which discontinuities were not observed within this region of individual experimental wings, the *cut* wing phenotype was considered suppressed. Conversely, in cases in which discontinuities were observed, regardless of the number of bristles affected, the *cut* wing phenotype was considered not suppressed. The scoring system is based on "all or none" suppression and therefore does not take into account individual variation in either the frequency or the severity of margin bristle loss of individual wings. The degree of penetrance correlated well with the degree of severity. In Table 2, "suppression of *ct*^{K}" was calculated for each genotype by dividing the number of wings suppressed by the total number of wings scored. The ability of deficiency chromosomes to affect *ct*^{K} and *ct*^{53d} was scored in a similar manner. To quantify phenotypes, dissected wings of each genotype were dehydrated in absolute ethanol, mounted in Canada Balsam:methyl-salicylate (1:3), and photographed at 10× magnification using a digital camera (Canon Power Shot S45) mounted on a compound microscope (Zeiss, Axioplan). For each genotype, a representative image of a median wing phenotype was selected from a photographic series.

Molecular analysis of GS vector insertion lines: Genomic sequences flanking the 5′-end and/or the 3′-end of the GS vector insertions were recovered by inverse PCR. Total DNA isolated from individual GS vector insertion lines was digested with *Sau*3AI (with 5′ primer set) or *Msp*I (with 3′ primer set) and ligated under dilute conditions according to the protocol available from the Berkeley *Drosophila* Genome Project. Genomic DNA immediately flanking the 5′- and 3′-ends of the GS

vector was amplified by PCR using the following GS-vector-specific primer sets: GS[5′] (GS[5′R]—5′-CCG TAG ACG AAG CGC CTC TAT TTA TAC T-3′ and GS[5′L]—5′-CCT CTC AAC AAG CAA ACG TGC ACT GAA) and GS[3′] (GS[3′R]—5′-CGC TGT CTC ACT CAG ACT CAA TAC GAC A-3′ and GS[3′L]—5′-GCT TAG CTT TCG CTT AGC GAC GTG TTC A-3′). PCR products were sequenced using the GS[5′L] or GS[3′R], as used in the initial amplification reaction. Sequence analysis was performed using the BLASTN program administered by the National Center for Biotechnology. This allowed GS vector insertion sites to be precisely located and known or predicted genes immediately flanking the insertion site to be identified. The Apollo Genome Annotation and Curation Tool, Version 1.3.5 (Lewis *et al.* 2002) was used to establish the proximity of individual GS insertions to flanking genes. The GS vector insertion site was determined for 66 of 79 GS lines that suppressed the ct^K phenotype. The "locus" heading in Table 2 represents the known or predicted gene closest to and downstream of the GS insertion.

***In situ* hybridization, immunohistochemistry, and X-Gal staining:** *In situ* hybridization to third instar wing discs was performed as described by Sturtevant *et al.* (1993) using digoxigenin (DIG)-labeled RNA probes and visualized using alkaline phosphatase conjugated α-DIG antibody (Roche; 1:200). To generate *lola* and *pipsqueak* (*psq*) RNA probes, coding DNA sequences from both loci were amplified by PCR using gene-specific primer sets *lola[766bp]* (*lola[A]*—5′-GTC CTC GTC ATC GCC TTG-3′ and *lola[B]*—5′-GAA CAG TAC GAC AAA CAT CC-3′) and *psq[644bp]* (*psq[A]*—5′-GTA GCG ATA GCG TGC CAG-3′; and *psq[B]*—5′-GCT GCT GAA ACA CGG ACG-3′)]. PCR products were cloned into the pGEM-T Easy Vector (Promega, Madison, WI). Immunohistochemistry on third instar wing discs was performed according to standard techniques. Dissected third instar wing discs were fixed with 4% formaldehyde/$NaPO_4$, washed with PBS/0.5% Triton X-100 (PBST), and blocked with PBST/4% BSA. Antibodies were used at the following dilutions: α-Wg (1:50; 4D4, Developmental Studies Hybridoma Bank), α-Ct (1:20; 2B10, DSHB), α-βGal (1:40; 40-1a, DSHB), and horseradish peroxidase conjugated α-mouse (1:200; Bio-Rad, Richmond, CA). *In situ* detection of β-galactosidase activity in dissected third instar wing imaginal discs was carried out as described by Glaser *et al.* (1986).

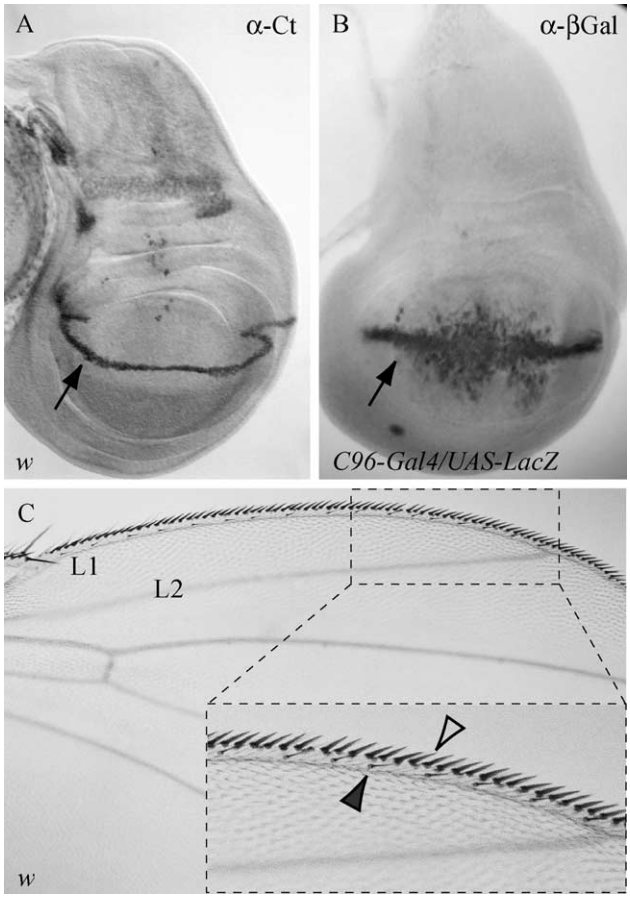

Figure 1.—Cut is expressed in the wing margin and is required for the development of the margin sensory bristles. (A) In the third larval instar wing disc, Cut is expressed in a stripe of cells 3–4 cells wide (arrow), corresponding to the Wg organizer. These Cut-expressing cells are the precursor cells of the stout and slender margin mechanosensory bristles. (B) *C96-Gal4* drives expression in a pattern overlapping the Cut-expressing cells. (C) The anterior wing margin, delimited by the L1 wing vein, is composed of a triple row of sensory bristles. Positioned on the dorsal wing surface is a single row of slender-shaft recurved chemosensory bristles (inset, solid arrowhead) adjacent to a row of stout-shaft mechanosensory bristles (inset, open arrowhead). Ventral and out of the plane of focus is the third bristle row composed of slender mechano- and chemosensory bristles.

RESULTS

Cut is required independently of Wingless maintenance to specify wing-margin sensory organs: The presumptive wing margin of the third instar larval wing disc consists of a stripe of Cut-expressing cells located at the dorsal/ventral boundary, a region corresponding to the Wg organizer (Figure 1A). Patterning of the wing margin, which contains an organized array of chemosensory and mechanosensory bristles (Figure 1C), is regulated in part by the secreted morphogen, Wg (Phillips and Whittle 1993; Johnston and Edgar 1998; Johnston and Sanders 2003; Duman-Scheel *et al.* 2004). Cut activity is required to maintain Wg expression in the presumptive wing margin, which otherwise degenerates cell nonautonomously. Since degeneration of wing tissue prefigures the development of the margin sensory bristles, it has been difficult to resolve the autonomy of Cut function in margin sensory organ specification. To determine a Wg-independent requirement for Cut in wing-margin development, we prevented degeneration of margin tissue in *cut* mutants by (1) maintaining Wg expression ectopically and (2) preventing apoptotic cell death through the misexpression of the baculovirus caspase inhibitor p35.

The ct^K, ct^6, and ct^{2s} alleles display a *cut* wing phenotype characterized by incised wing-blade tissue and decreased numbers of margin bristles (Figure 2, A–C). Whereas the ct^K allele primarily disrupts margin bristle development, ct^6 and ct^{2s} disrupt both blade tissue and margin bristle development. The margin-specific overexpression of *UAS-cut* directed by the *C96-Gal4* driver significantly rescues the *cut* wing phenotype (Figure 2, D–F). In hemizygous ct^K/Y mutant males, the large dis-

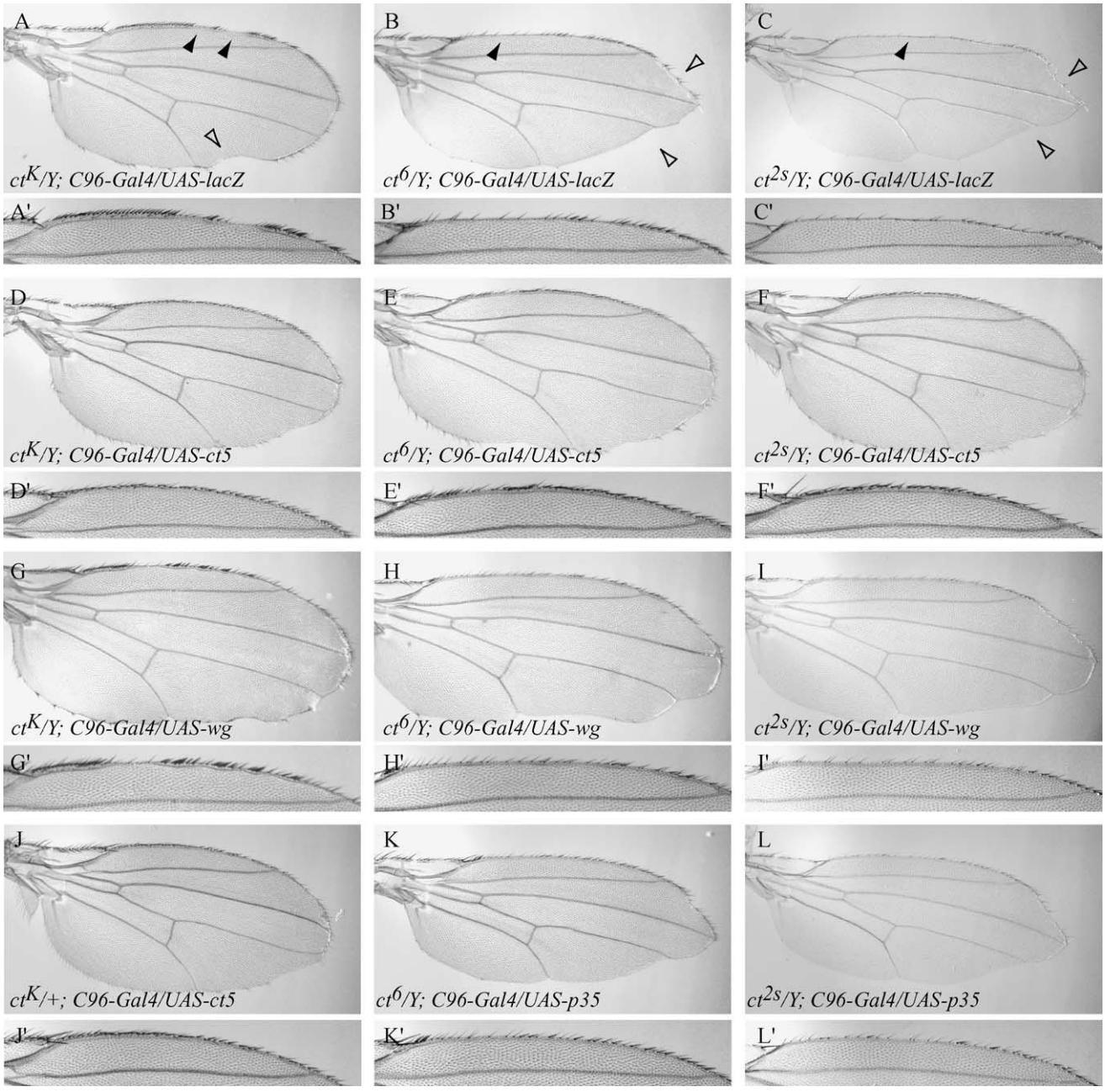

Figure 2.—The requirement for *cut* in patterning the wing margin is independent of its role in maintaining Wg expression. All genotypes were reared at 25°, excepting G–I, which were raised at 18°. (A–C) The Lethal I *cut* allele, ct^K, and the two *cut* alleles, ct^6 and ct^{2s}, display large discontinuities in the margin bristles (solid arrowheads), in addition to incised margin and blade tissue (open arrowheads). (D–F) *C96-Gal4*-directed overexpression of *UAS-ct5* suppresses the wing defects in *cut* mutants. Although the large discontinuities in the anterior margin bristles of ct^K are suppressed, the total number of sensory bristles is only partially restored, likely reflecting a dominant Cut misexpression phenotype (see J). (G–I) Overexpression of *UAS-wg* suppresses the degeneration of wing-blade tissue in *cut* mutants, but is unable to restore margin bristles. (J) The overexpression of *UAS-ct5* in heterozygous ct^K females disrupts anterior margin bristle development. A similar effect was observed in wild-type individuals. (K and L) Blocking apoptosis by overexpression of *UAS-p35* partially suppresses the loss of blade and margin tissue, but is unable to suppress the loss of margin bristles.

continuities in the regular array of anterior margin bristles are rescued by Cut overexpression, but the total number of margin bristles remains less than that of wild type (Figure 2D). This may be interpreted as an incomplete rescue. However, since a similar reduction in margin bristle number is observed when Cut is overexpressed in heterozygous ct^K/+ females (Figure 2J), which under normal conditions have wings of wild-type

TABLE 1

Rescue of anterior wing-margin sensory bristles

	Crossed to:			
	ct^{2s}; C96-Gal4		*ct^{6}; C96-Gal4*	
	Stout-shaft	Slender-shaft	Stout-staft	Slender-shaft
UAS-lacZ	7.7 ± 0.6 (n = 15)	21.7 ± 0.6 (n = 15)	12.2 ± 0.7 (n = 19)	22.3 ± 0.6 (n =1 9)
UAS-p35	9.9 ± 0.5 (n = 15)**	28.1 ± 0.7 (n = 15)***	16.1 ± 0.9 (n = 15)***	28.8 ± 0.6 (n = 15)***
UAS-wg	6.6 ± 0.6 (n = 11)	40.1 ± 0.8 (n = 11)***	10.0 ± 3.0 (n = 2)	43.5 ± 2.5 (n = 2)***
UAS-ct5	35.4 ± 4.0 (n = 9)***	35.6 ± 3.1 (n = 9)***	40.9 ± 1.8 (n = 14)***	43.7 ± 1.8 (n = 14)***
$lola^{GS[A916]}$	34.0 ± 1.3 (n = 16)***	35.4 ± 1.5 (n = 16)***	35.9 ± 2.9 (n = 9)***	37.4 ± 1.5 (n = 9)***

Summation of dorsal and ventral slender-shafted mechano- and chemosensory bristles and stout-shafted mechanosensory bristles located within the region stretching from the hinge-proximal anterior wing margin to the L1/L2 wing-vein intersect. Standard error of mean is given. Wild-type wings display an average of 68.8 ± 0.6 dorsal and ventral slender bristles and 69.8 ± 0.6 stout-shafted bristles. Statistical significance was determined using Student's *t*-test; **, $P < 0.01$; ***, $P < 0.001$. Although there is some evidence of improvement in slender bristle number resulting from the misexpression of either *UAS-p35* or *UAS-wg* misexpression, the number of stout bristles is only minimally affected in either instance.

morphology, we prefer the alternative interpretation that a complete rescue is confounded by a dominant negative effect resulting from Cut overexpression (see also Ludlow *et al.* 1996). Cut overexpression also partially restores blade tissue and margin bristles of the ct^6 and ct^{2s} alleles (Figure 2, E and F). In particular, the number of stout mechanosensory bristles is significantly rescued (Table 1).

Ectopically supplying Wg in the presumptive wing margin of ct^K, ct^6, and ct^{2s} mutants also suppresses the loss of wing-blade tissues, including the slender recurved chemosensory bristles, but does not rescue the loss of the stout mechanosensory bristles (Figure 2, G–I, and Table 1). In several hypomorphic *cut* mutations, although Cut expression is disrupted in the mechanosensory and non-innervated bristles of the wing margin, expression in the precursor cells of the slender chemosensory bristles is unaffected (Jack *et al.* 1991). It has been proposed that loss of Cut expression in the wing margin results in the failure of the mechanosensory and non-innervated bristles to differentiate, followed by the cell nonautonomous degeneration of the margin. Therefore, it is possible that the loss of the slender chemosensory bristles is a secondary effect resulting from degeneration of the margin, rather than a cell autonomous effect resulting from the loss of Cut expression. We propose that by ectopically expressing Wg in *cut* mutants we suppress the degeneration of wing-margin tissue, which includes the slender chemosensory bristles, resulting from the failure of Cut-dependent maintenance of Wg expression. Only those cells that actually fail to express Cut (*i.e.*, the precursor cells of the stout mechanosensory bristles) fail to be rescued by the misexpression of Wg. Thus, we propose that Wg is unable to promote sensory bristle development independently of Cut function and suggest that Cut is required autonomously for sensory bristle specification in a manner independent of its role in maintaining Wg expression. However, the possibility that a Wg signal, in addition to Cut activity, is required for margin bristle specification cannot be excluded.

Gain- and loss-of-function suppressor screens of the *cut* wing phenotype: Having determined the dual requirement of *cut* to maintain margin cell survival and to specify margin bristle identity, we carried out complementary loss-of-function and gain-of-function suppression screens of the ct^K phenotype to identify genes that interact with *cut* during wing-margin patterning. ct^K is classified as a Lethal I *cut* allele, as defined by its failure to complement all *cut* mutant alleles except for the *kinked femur* class (Jack 1985). Placed in *trans* to a *cut* null allele, ct^K is characterized by both semilethality and the transformation of embryonic ES organs into chordotonal organs. Unlike other Lethal I alleles, however, adult males that are hemizygous for the ct^K allele are viable and display a completely penetrant *cut* wing-margin phenotype (Figure 2A). Because of these characteristics, we reasoned that ct^K would provide a uniquely sensitized background in which genetic suppressor screens could be designed to identify genes involved in both wing-margin patterning and sensory bristle specification.

In an initial approach, we carried out a dominant loss-of-function suppression screen using available cytological deficiencies covering ~50% of the genome. Male flies from each deficiency line were crossed to females homozygous for ct^K, and the *cut* wing phenotype of the resulting male progeny—hemizygyous for ct^K and heterozygous for the deficiency chromosome—was scored. The capacity of each deficiency chromosome to dominantly suppress ct^K was quantitatively assessed according to their ability to reduce the overall penetrance of ct^K-associated discontinuities in the anterior wing-margin sensory bristles (materials and methods). The results of this screen are summarized in Table 2. *Df(2L)Prl*, *Df(3L)Cat*, and *Df(3R)p25-Df(3R)P2* completely sup-

TABLE 2

Summary of gain- and loss-of-function GS vector insertion lines and deficiency chromosomes: molecular data and genetic interactions with *cut*

Locus[a]	Cytology	Insertion-site flanking sequence[b]	GS vector insertion	Molecular function/domain structure	Suppression of $ct^{K\,c}$ (%)	Genetic interactions: *cut* wing alleles[d]
			Gain-of-function GS vector lines			
lola[e]	47A11-13	ACGCTTTTTTCCAACGAGAC_	GS[A916]	Transcription factor/zinc finger/BTB domain	94	Group A (ct^{6}, ct^{53d}, ct^{2s} sup.)
brat	37C1-6	TCCTCTCGAAAGTTCTGCGG_	GS[A2233]	Transcription factor/B-box zinc finger	77	Group A (ct^{53d} sup.)
CG14757	44B9	AACTCGAACTCACACCAAAC_	GS[A2066]	—	60	Group A (ct^{53d} sup.)
CycE	35D	AGTGAAGGAAAGAGCGGGAG_	GS[A1869]	Cyclin-dependent protein kinase regulator	4	Group A (ct^{53d} sup.)
CG12340[d]	47C1	GTCTTCGTCG _(TTTAAGGG)^{9}CA	GS[A2450]	—	~*ct* rescue	Group B (ct^{53d} enh.)
squeeze (*sqz*)	91F8-9	_TGTCGCCCCCAACAAAAGAG	GS[A2967]	Transcription factor/zinc finger	~*ct* rescue	Group B (ct^{53d} enh.)
eukaryotic initiation factor 4E (*eIF-4E*)[e]	67B3	_CGCATACCACACGTTTTCAG	GS[A2783]	Translation initiation factor	55	Group B (ct^{53d} enh.)
eukaryotic initiation factor 4a (*eIF-4a*)	26B2	_GTTCACACGCTGCGGTAAAA	GS[A2207]	Translation initiation factor/ DEAD-box/helicase	49	Group B (ct^{53d} enh.)
Adult enhancer factor 1 (*Aef1*)	78D2	GCCACAGATAATGCTGTGAG_	GS[A2724]	Transcription factor/zinc finger	45	Group B (ct^{53d} enh.)
lesswright (*lwr*)	21E1	_AGTGAGACCCTTTGTGTAGA	GS[A2612]	Ubiquitin-like conjugating enzyme	35	Group B (ct^{53d} enh.)
fusilli (*fus*)	52B3-5	ATAAGCGGCCCACGCACACC_	GS[A1497]	EGFR-signaling pathway/RNA binding	22	Group B (ct^{53d} enh.)
posterior sex combs (*psc*)	49E6	_GGCCGAGCCACGACGACACG	GS[A2026]	Chromatin-remodeling/RING finger domain	16	Group B (ct^{53d} enh.)
CG5390	31D1	_GGCTGAGACTTAAGATTGAA	GS[A2688]	Serine protease	11	Group B (ct^{53d} enh.)
Sphingomyelin synthase-related (*SMSr*)	65F7-9	_CTCTGAACGGAACAACTGAG	GS[A2330]	Sphingomyelin biosynthesis	8	Group B (ct^{53d} enh.)
chickadee (*chic*)	26A5-B2	TCAAAATCGGTTTATGGTTC_	GS[A2665]	Cytoskeleton constituent/ actin-binding domain	7	Group B (ct^{6} sup./ct^{53d} enh.)
apontic (*apt*)[e]	59F1-4	ATTGTCATTA_(CTTTTGGC)^{9}CC	GS[A960]	Transcription factor/Myb domain	~*ct* rescue	Group C (ct^{K} sup.)
hairy (*h*)	66D1	TATATATAGCGCAACCATCC_	GS[A1546]	Transcription factor/HLH dimerization domain	~*ct* rescue	Group C (ct^{K} sup.)
hephaestus (*heph*)	100D3-E1	_ATCCAGCGGAAAGAGAGCGG	GS[A1768]	Polypyrimidine tract binding	~*ct* rescue	Group C (ct^{K} sup.)
CG7752	78C4-5	TCCGTCGAGAACTGCTACAG_	GS[A1165]	Transcription factor/zinc finger	61	Group C (ct^{K} sup.)
G protein α-subunit 65A (*G-iα65A*)	65D5	_ATTCCGGTATTTCCCCCCTT	GS[A2888]	Guanine-nucleotide-binding protein, α-subunit	37	Group C (ct^{K} sup.)
CG30497	43E13-16	_GCACGGAACGTAGAACGCAG	GS[A1957]	—	25	Group C (ct^{K} sup.)
CG10373	37A1	CATTGCTTGTTAGTCAGCAC_	GS[A1703]	Amino acid transport	25	Group C (ct^{K} sup.)
Ssl1	80B2	_AGCCGGCGCATTTTATTTAG	GS[A1702]	Transcription factor/TFIIH complex	23	Group C (ct^{K} sup.)

(*continued*)

TABLE 2

(Continued)

Locus[a]	Cytology	Insertion-site flanking sequence[b]	GS vector insertion	Molecular function/domain structure	Suppression of ct^{K} [c] (%)	Genetic interactions: *cut* wing alleles[d]
schnurri (*shn*)	47D6-E1	_ACTATAAGTTAGCAAACAAA	GS[A2114]	Transcription factor/zinc finger	17	Group C (ct^{K} sup.)
CG31782	36A10-12	_GTCCGAAGGCTTATACAGAA	GS[A2197]	Transcription factor	13	Group C (ct^{K} sup.)
CG1888	45F1	_AATGTCTACATACGCGTACA	GS[A2442]	—	10	Group C (ct^{K} sup.)
CG7920	99D1	_GGCGAACCAGTTGCAAATTT	GS[A828]	Acetyl-CoA hydrolase/ transferase	7	Group C (ct^{K} sup.)
regular (*rgr*)	44D4	GTAAGTTAATCACCGCCGCC_	GS[A1998]	Transcription factor/zincfinger	6	Group C (ct^{K} sup.)
Activin like protein at 23B (*Alp23B*)	23B1-2	_GTCTATAGTCATAAATCGAG	GS[A1800]	Signaling ligand/TGFβ-like	4	Group C (ct^{K} sup.)
anterior open (*aop*)	22D1	GCTCCGCTTTACGGCTGGCA_	GS[A1685]	Transcription factor/ Et-domain	4	Group C (ct^{K} sup.)
Serine palmitoyltransferase subunit I (*Spt-I*)	49F4	GATATTTCACGCCTTTTGCC_	GS[A2040]	Aminotransferase/ pyridoxal 5′-phosphate (PLP)-dependent transferase	4	Group C (ct^{K} sup.)
trx	88B1	_GTTAGAATTTTCGTTTATCT	GS[A2270]	Chromatin-remodeling/PHD domain	4	Group C (ct^{K} sup.)
14-3-3ζ	46E6-8	GTTAAGTTGTAGGCGCGGAC_	GS[A2789]	Protein kinase C inhibitor	4	Group C (ct^{K} sup.)
CG15236	42D4-6	ATGAATGCCAGACCCAGAGC_	GS[A2203]	–	4	Group C (ct^{K} sup.)
CG17075	21B6-7	TACGAACCTATAACTGCGCC_	GS[A1942]	–	3	Group C (ct^{K} sup.)
		Loss-of-function GS vector lines				
mor	89A11	_GATTCGCCAGTGGCTGCAGA	GS[A897]	Chromatin-remodeling/Myb domain	79	Group B (ct^{53d} enh.)
Vha68-2	34A3	GAGAAAAGCAGCAATCACAC_	GS[A1548]	Cation transport	24	Group B (ct^{53d} enh.)
thioredoxin-2 (*Trx-2*)	30C1	_GATGTGCCAATCGGTCAATC	GS[A866]	Thiol-disulfide exchange intermediate	40	Group C (ct^{K} sup.)
CG6907	25E5	_GTGTGCCCCCATTGGCAGCC	GS[A945]	—	28	Group C (ct^{K} sup.)
CG9270	38F6	_CCTCGGGCACTCCGTAAACG	GS[A839]	ABC transporter	16	Group C (ct^{K} sup.)
mitochondrial ribosomal protein L4 (*mRpL4*)	35F11	ACATTTTTCG_(TGTCACGG)^{2}TG	GS[A961]	Mitochondrial large ribosomal subunit	14	Group C (ct^{K} sup.)
stathmin (*stai*)	26B9	AAGCCCAGCTGGTGCTCACC_	GS[A1533]	Microtubule-associated protein	8	Group C (ct^{K} sup.)
		Deficiency chromosomes				
Df(2L)Prl	32F-3; 33R1-2				100	ND
Df(3L)Cat	75C1-2; 75F1				100	ND
Df(3R)p25, Df(3R)P2	85A3; 85B1, 89D9-E1; 89E2-3				100	ND

(*continued*)

pressed ct^K. Unlike the *Df(3R)p25-Df(3R)P2* dual deficiency chromosome, neither *Df(3R)p25* nor *Df(3R)P2* alone was able to suppress ct^K. It is possible that the two deficient genomic regions cooperate to suppress ct^K, or an unrelated second-site mutation present only in the dual deficiency may be responsible for the suppression. A fourth deficiency, *Df(3R)sbd105*, partially suppressed ct^K as assessed by a decrease in the severity of margin bristle loss, but did not reduce the overall penetrance of the phenotype. *Df(3R)sbd105* covers *moira* (*mor*), a gene encoding a core subunit of the Brahma (BRM) chromatin-remodeling complex. Genetic interactions between *cut* and components of the BRM complex are examined below.

The ct^K allele results from the insertion of a gypsy retrotransposon into the *cut* locus ~6 kb upstream of the first exon, where it partially disrupts the regulation of embryonic and adult Cut expression (Jack 1985; Jack and DeLotto 1995). In wing tissue, the gypsy element functions by insulating the activity of the distal wing-margin enhancer from the proximal promoter, resulting in the loss of Cut expression specifically in the wing margin. At least two genes are known to be directly required for gypsy-mediated gene insulation: *Suppressor of Hairy wing* [*Su(Hw)*] and *modifier of mdg 4* [*mod(mdg4)*] (Hoover *et al.* 1992; Gause *et al.* 2001; Ghosh *et al.* 2001). The ct^K allele is unusual in that it contains a mutated gypsy insulator with a partial deletion of the Su(Hw)-binding region, which presumably makes it more sensitive to moderate decreases in the activity of Su(Hw) and mod(mdg4) (Hoover *et al.* 1992). As part of the deficiency screen, two deficiencies, *Df(3R)red1* and *Df(3R)e-N19*, respectively covering *Su(Hw)* and *mod(mdg4)*, were tested for an interaction with ct^K. Although loss-of-function mutations in both genes have been shown to dominantly suppress ct^K (Hoover *et al.* 1992; Gause *et al.* 2001), our screen failed to identify either deficiency. In the case of *mod(mdg4)*, however, mutations that suppress ct^K behave as antimorphic alleles in that they suppress the wing phenotype more strongly than null alleles do. This could account for why we did not identify *Df(3R)e-N19* as a dominant suppressor of ct^K. Similarly, the chromosome deficiencies *Df(2R)vg*-B, *Df(2R)Px4*, and *Df(2R)nap1*, covering loci previously shown to encode positive regulators of Cut expression and including the genes *vestigial*, *Chip*, and *Nipped-B*, respectively, were tested for an interaction with ct^K. Only *Df(2R)nap1* showed an interaction in the wing. *Df(2R)nap1* enhanced the wing phenotype of hemizygous ct^K males and produced a mild dominant *cut* wing phenotype in heterozygous ct^K females. This is consistent with previous evidence suggesting that Nipped-B facilitates the activation of *cut* expression (Rollins *et al.* 1999, 2004). Deficiencies covering other regulators of *cut* expression, including *scalloped* and *mastermind*, were not tested (Morcillo *et al.* 1996).

We also conducted a complementary gain-of-function screen using the modular GS system of misexpression (Toba *et al.* 1999). The margin-specific Gal4 driver, *C96-Gal4*, was used to drive expression of genes located proximal to 2066 unique insertions of the GS vector (materials and methods). The ability of individual GS lines to suppress ct^K was scored as described above. In total, 3.8% of the GS vector insertions (79/2066), representing at least 42 distinct loci, were found to suppress the ct^K phenotype (Table 2). Insertions at 35 loci suppressed the ct^K phenotype in response to Gal4-dependent misexpression. The seven remaining loci suppressed without the *C96-Gal4* driver and presumably act as dominant loss-of-function suppressors of ct^K. In addition, a large number of gain-of-function GS lines (319/2066) enhanced the ct^K phenotype, as determined by an increase in the severity of margin tissue loss. Due to the large number of ct^K-enhancing loci, we opted not to characterize them further and instead focused on the suppressing loci.

As previously stated, it is possible that genes identified by the ability to suppress ct^K may result from an interaction with the *cut* regulatory region or, alternatively, with the gypsy insulator or a gene required for gypsy insulator activity. To distinguish between these possibilities and to further characterize the interaction with *cut*, we examined the ability of the candidate GS suppressor lines to modify the wing phenotype of the weak ct^{53d} allele. In contrast to ct^K, the ct^{53d} allele results from a partial deletion (~500 bp) of the minimal *cut* wing-margin enhancer (defined as a region of ~2.7 kb) and does not contain gypsy-derived elements (Jack *et al.* 1991;

TABLE 2

(Continued)

ND, not determined.

[a] Gene or predicted gene located closest to the insertion site and positioned in the 5′–3′ orientation relative to the GS vector.

[b] Genomic sequence of the coding strand (5′–3′ orientation) flanking the site of GS vector insertion (underscore).

[c] GS insertion lines were crossed to ct^K*; C96-Gal4* females. Male progeny of the genotype ct^K*/Y; GS*[#]*/C96-Gal4* were scored. The percentage of suppression is equal to the number of wings displaying a complete suppression of ct^K-associated gaps in the anterior margin sensory bristles divided by the total number of wings scored. Cases in which ct^K suppression resembled the dominant phenotype resulting from the overexpression of Cut are represented by "~*cut* rescue." The suppression of ct^K for all GS vector insertion lines is significant ($P \leq 0.01$). Less than 1.0% of negative control males (ct^K*/Y; UAS-lacZ/C96-Gal4*) were suppressed.

[d] Genetic interactions with *cut* wing alleles ct^6 (gypsy), ct^{53d} (non-gypsy), and ct^{2s} (non-gypsy) are summaried.

[e] Multiple unique GS vector insertions were identified within locus.

Mogila *et al.* 1992). The ct^{53d} allele disrupts Cut expression primarily in the presumptive wing tip, which corresponds to a severe loss of wing tissue in the distal-most region of the adult wing. The genetic interaction data with ct^{53d} are summarized in Table 2.

Candidate suppressor loci were classified into three groups according to the genetic interaction with ct^K and ct^{53d}. Group A loci suppress both ct^K and ct^{53d} and are expected to represent candidate regulators or effectors of *cut* activity. The interaction with ct^{53d} indicates that group A loci do not suppress the ct^K wing phenotype simply by interfering with gypsy activity. In contrast, group B loci suppress ct^K and enhance ct^{53d}, suggesting a more complex interaction with the *cut* locus during wing-margin patterning. This may include direct interference with gypsy insulator activity, in addition to being required for *cut* wing enhancer activity. It should be noted that all group B loci, except a subgroup that suppressed the ct^K equivalent to the UAS-Cut rescue, do not adversely affect wing development when misexpressed in heterozygous *cut* mutant females. Thus, enhancement of the wing phenotype in hemizygous ct^{53d} mutant males is unlikely due to misexpression alone. Finally, group C includes candidate loci that suppress only ct^K and are therefore presumed to interfere with gypsy activity. For instance, one gain-of-function suppressor contains a GS insertion near *trithorax* (*trx*), a gene previously shown to enhance gypsy insulator activity when mutated (Gerasimova and Corces 1998).

Group A consists of four candidate loci that suppress both ct^K and ct^{53d} and includes *brain tumor* (*brat*), *CyclinE* (*CycE*), and *lola*. *brat* encodes a tumor-suppressor protein (Frank *et al.* 2002) and *CycE* a cell cycle regulator controlling the G_1/S phase transition (Richardson *et al.* 1993, 1995). Thus, both may act to suppress the wing phenotype by influencing cell growth and proliferation. The genetic interaction with *lola* is explored further below.

Group B consists of 12 candidate loci, including two genes encoding components of the eukaryotic translation initiation factor 4F complex (eIF-4F), *eIF-4A* and *eIF-4E* (reviewed in Gebauer and Hentze 2004). eIF-4A and eIF-4E regulate translation downstream of the insulin/target of rapamycin signaling pathway and as such act globally to regulate cell growth and proliferation (Miron *et al.* 2003). Overexpression of eIF-4E and eIF-4A may relieve putative cell growth or survival deficits associated with the loss of *cut* activity by enhancing the translation of Cut target genes. Similarly, group B candidate genes *lesswright* (*lwr*) and *fussilli* (*fus*) are also involved in regulating cell growth or proliferation of wing imaginal tissue. Some heterozygous mutants of *lwr*, a gene encoding a ubiquitin-like conjugating enzyme, exhibit wings severely reduced in size (Epps and Tanda 1998). Lwr has been shown to be required for the nuclear import of Bicoid during early embryogenesis (Epps and Tanda 1998). It is possible that Lwr plays a role in the nuclear import of Cut or its downstream targets. The RNA-binding protein Fus is involved in regulating cell growth in the wing disc and, similarly to eIF-4F, may affect the translation of Cut target genes (Wakabayashi-Ito *et al.* 2001; Raisin *et al.* 2003). The differential interaction of group B candidates with various *cut* alleles likely reflects either direct or indirect effects on both gypsy insulator activity and *cut* wing-enhancer-mediated transcription. It will be of interest to determine if group B loci regulate gene insulation and transcription via common mechanisms.

A subgroup of gain-of-function candidate genes, including *Hephaestus* (*heph*), suppress the ct^K wing-margin patterning defects to a degree comparable to the UAS-Cut rescue; the large discontinuities in the triple-row bristles are mitigated, but the total number of sensory bristles is less than normal. Heph is expressed in the presumptive wing and encodes a polypyrimidine tract binding protein that binds to and regulates RNA stability (Dansereau *et al.* 2002). Heph appears to attenuate Notch signaling downstream of the binding of the Notch ligand, Delta, and $heph^-$ clones cause the nonautonomous formation of wing-margin structures (Dansereau *et al.* 2002). How the overexpression of Heph and presumably the attenuation of Notch signaling suppresses ct^K is not clear. It is possible that Heph may affect the activity of the gypsy insulator, since overexpression of Heph did not produce an appreciable alteration of the ct^{53d} wing phenotype.

***longitudinals lacking* is required for *cut*-dependent wing-margin patterning:** Twenty-one GS vector lines with insertions at 12 unique locations proximal to the coding region of *lola* were identified by their ability to suppress the ct^K allele ($lola^{GS[A916]}$; Figure 3, A and B). All $lola^{GS}$ insertions require the *C96-Gal4* driver, indicating that suppression results from GS-vector-mediated overexpression. $lola^{GS[A916]}$-mediated suppression of the ct^K phenotype is robust with 94% of ct^K mutant wings displaying a normal triple row of sensory bristles (Table 2). The ct^{53d}, ct^6, and ct^{2s} alleles are also strongly suppressed by $lola^{GS[A916]}$ (Figure 3, C–H, and Table 1), demonstrating that the interaction with *cut* in the wing margin is not allele specific. In addition to reversing the loss of sensory bristles, $lola^{GS[A916]}$ suppresses the loss of blade tissue, a phenotype thought to result from a failure of Cut to maintain Wg expression (Micchelli *et al.* 1997). $lola^{GS[A916]}$ may interact with *cut* both during Wg-dependent patterning of the wing margin and during the specification of margin bristles.

lola and its neighboring gene *psq* are both positioned in the proper orientation to be overexpressed by insertions of the bidirectional GS vector proximal to the 5′ region of *lola*. Using *in situ* hybridization with both *lola*- and *psq*-specific RNA probes, we found the expression of both genes to be elevated in wing imaginal discs in response to *C96-Gal4*-driven overexpression of the $lola^{GS[A916]}$ line (Figure 4, A and B). However, semiquantitative RT-PCR revealed that only *lola* mRNA transcripts

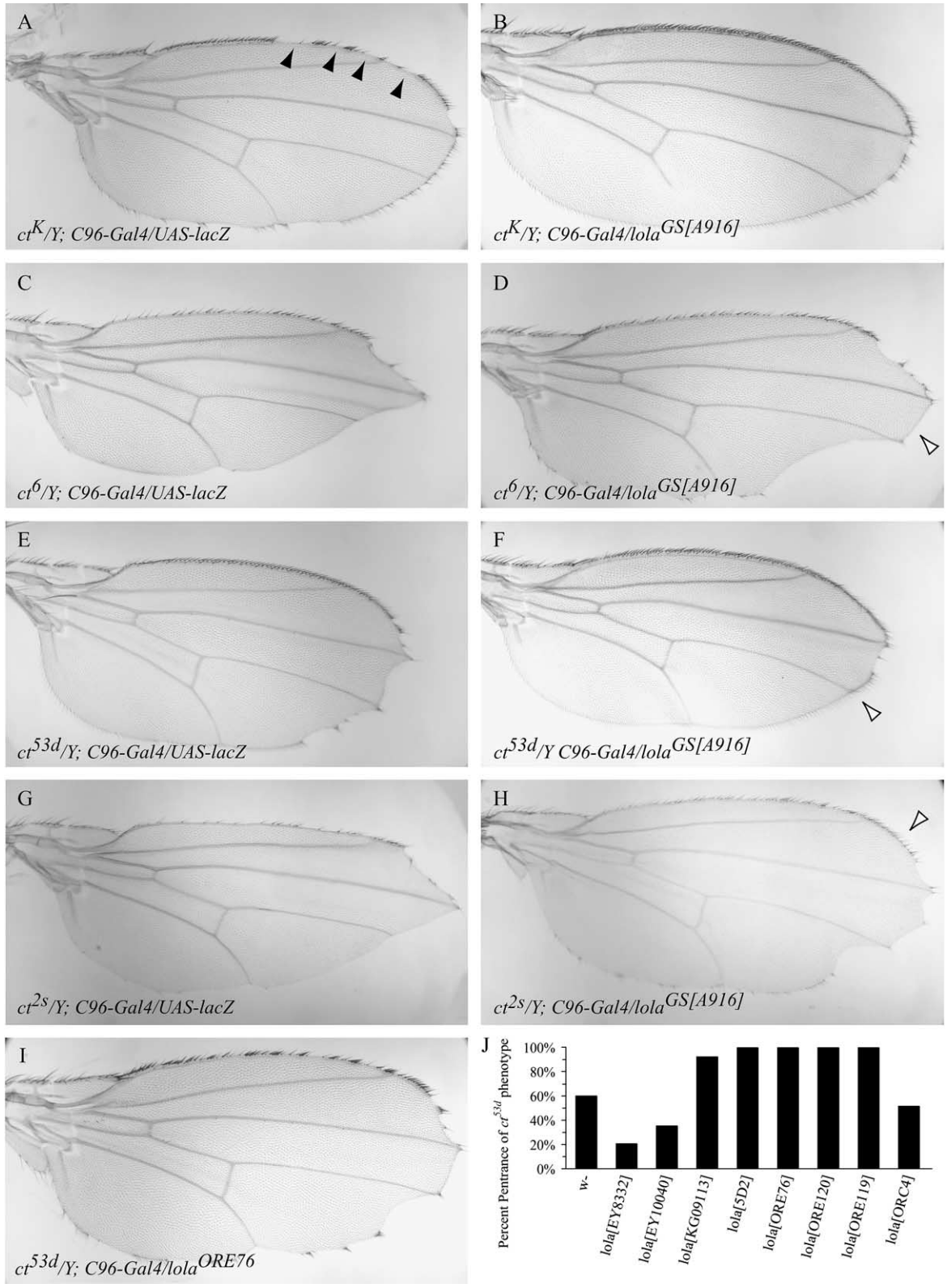

Figure 3.—*lola* interacts genetically with *cut* during wing-margin development. (A–H) The overexpression of *lola*$^{GS[A916]}$ can suppress the wing phenotype of ct^K (B), ct^6 (D), ct^{53d} (F), and ct^{2s} (H); compare to *UAS-lacZ* negative control wings (A, C, E, and G). Solid arrowheads in A represent discontinuities in the anterior wing margin; open arrowheads in D, F, and H represent rescue of margin tissues. (I and J) Loss-of-function *lola* alleles enhance sensory bristle loss in the anterior wing margin of ct^{53d}. (I) A single copy of the amorphic *lola*^{ORE76} allele aggravates the ct^{53d} wing phenotype (compare to E). (J) Penetrance of ct^{53d}-associated gaps in the sensory bristles of the anterior margin of wings heterozygous for various *lola* alleles. *lola*^{EY8332} and *lola*^{EY10040} are gain-of-function insertions of the EPgy2 *P* element; *lola*^{KG09113} is a loss-of-function insertion of the suppressor *P* element; *lola*^{5D2}, *lola*^{ORE76}, and *lola*^{ORE120} are amorphic alleles; and *lola*^{ORE119} and *lola*^{ORC4} are decision-selective alleles.

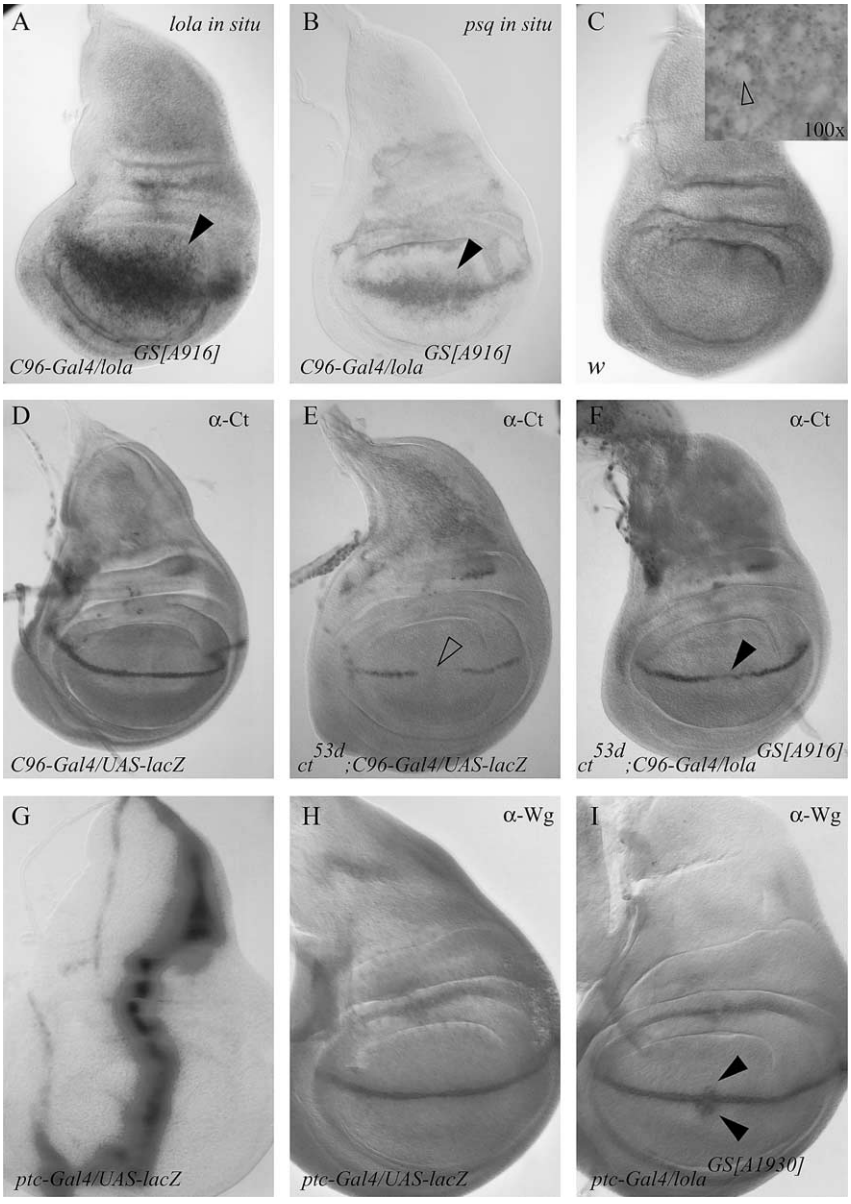

FIGURE 4.—Overexpression of *lola* in the wing imaginal disc rescues Cut expression and induces ectopic Wg expression. (A and B) *In situ* hybridization demonstrates that the expression of both *lola* and *psq* mRNA are induced in response to *C96-Gal4*-directed misexpression of $lola^{GS[A916]}$ (solid arrowheads). (C) *lola* mRNA is expressed ubiquitously in wild-type wing imaginal tissue. Staining is largely restricted to the cytoplasm of wing disc cells and excluded from the nuclei (inset, open arrowhead), indicting that the ubiquitous staining is not the result of nonspecific binding of the *lola* riboprobe. The *lola*-specific riboprobe used in A and C recognizes all *lola* mRNA isoforms. (D–F) Overexpression of $lola^{GS[A916]}$ rescues Cut expression in ct^{53d} mutant wing imaginal tissue. (D) In third instar wing imaginal disc tissue, wild-type Cut expression at the dorsoventral boundary is unaffected by a single copy of the *P{GawB}C96* insertion (*i.e.*, *C96-Gal4*). (E) Cut expression is reduced at the presumptive distal wing tip (open arrowhead) in ct^{53d} mutants. (F) *C96-Gal4*-directed overexpression of $lola^{GS[A916]}$ rescues Cut expression at the presumptive distal wing tip where Cut expression is normally lost in ct^{53d} mutants (solid arrowhead). (G and H) Overexpression of $lola^{GS[A916]}$ induces ectopic Wg expression. (G) *ptc-Gal4* drives expression along the anteroposterior axis of the wing disc. (H) The Wg expression domain overlaps that of Cut at the dorsoventral boundary. (I) *ptc-Gal4*-directed misexpression of $lola^{GS[A916]}$ results in ectopic Wg expression in cells adjacent to the dorsoventral boundary (solid arrowheads).

are consistently elevated in response to GS-vector-directed overexpression driven by heatshock-Gal4 (data not shown). Thus, suppression of the *cut* mutant wing phenotype is most likely due to the overexpression of Lola.

lola encodes a family of BTB-domain zinc-finger transcription factors previously shown to regulate multiple aspects of peripheral and central neuron axonal guidance (GINIGER *et al.* 1994; MADDEN *et al.* 1999; CROWNER *et al.* 2002). The *lola* locus is complex, encoding at least 20 different protein isoforms, each expressed in a partially distinct pattern (GOEKE *et al.* 2003; HORIUCHI *et al.* 2003). Seventeen of the isoforms each contain unique zinc-finger domains, indicating that each isoform may regulate a unique set of target genes. To determine if *lola* is involved in margin development, and if *lola* mutations interact with the *cut* locus, we examined the modifying effects of heterozygous *lola* loss-of-function alleles on the wing-margin phenotype of ct^{53d}. The amorphic *lola* mutations $lola^{ORE76}$, $lola^{ORE120}$, and $lola^{5D2}$ contain disruptions in the open reading frame of the N-terminal constant region present in all Lola isoforms and disrupt all known *lola* function (GOEKE *et al.* 2003). The presence of one mutant copy of $lola^{ORE76}$, $lola^{ORE120}$, or $lola^{5D2}$ results in a dramatic enhancement in the severity of the ct^{53d} phenotype in that the anterior margin bristles show multiple discontinuities (Figure 3, I and J). Wing-blade tissue adjacent to the area of missing margin bristles is minimally affected by *lola* mutations, indicating that margin cells with compromised *cut* activity have the greatest sensitivity to disruptions in *lola*. Of the decision-selective alleles, $lola^{ORE119}$, but not $lola^{ORC4}$, enhances the ct^{53d} phenotype (Figure 3J), implying that the interaction with *cut* in the wing margin is specific to certain Lola

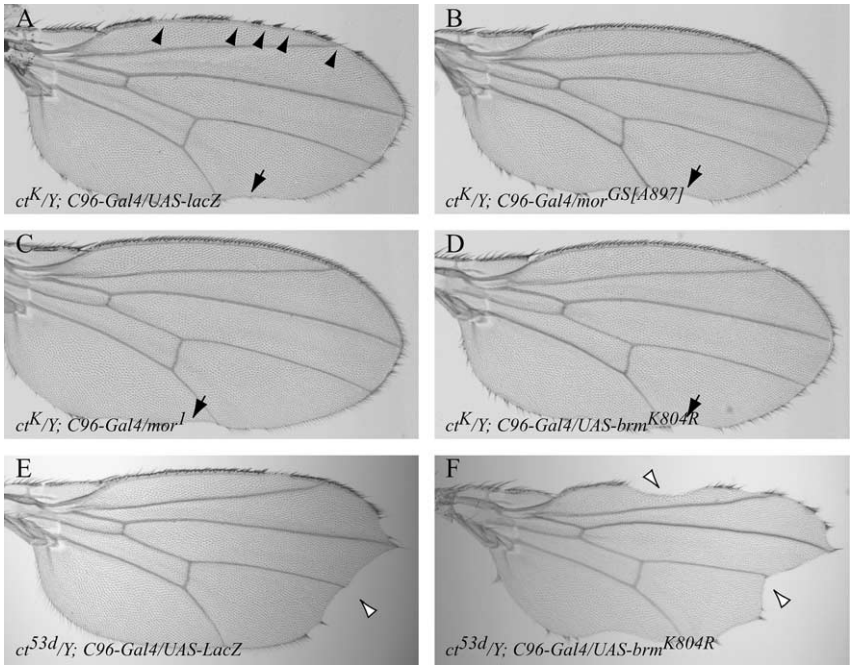

FIGURE 5.—The Brahma complex interacts genetically with *cut* during wing-margin development. (A–D) The ct^K-associated loss of margin bristles is suppressed by disrupting the Brahma complex subunits, Mor and Brm. (A) ct^K mutant wings consistently show numerous discontinuities in the stout mechanosensory margin bristles (arrowheads). (B and C) Heterozygous loss-of-function *moira* mutations, $mor^{GS[A897]}$ and mor^1, suppress completely the ct^K-associated loss of sensory bristles along the anterior wing margin. (D) Margin-specific overexpression of UAS-brm^{K804R} suppresses the ct^K wing phenotype in the anterior margin. *C96-Gal4*-directed overexpression of UAS-brm^{K804R} had no effect on wing development when misexpressed in an otherwise wild-type genetic background. Note that the posterior incisions of wing-blade tissue are not rescued by disrupting Mor or Brm function (arrows in A–D). (E and F) The ct^{53d} wing allele is differentially affected, as compared to ct^K, by the disruption of the Brahma complex activity. (E) The ct^{53d} wing phenotype is characterized by the severe loss of wing-blade tissue at the distal wing tip (open arrowhead) and by infrequent gaps in the anterior wing-margin sensory bristles. (F) The overexpression of UAS-brm^{K804R} enhances both the loss of wing-blade tissue (open arrowheads) and sensory bristles. Note that the anterior and posterior wing margin is similarly affected.

isoforms. In contrast to *lola*, loss-of-function *psq* alleles did not affect the ct^{53d} phenotype (data not shown). If *lola* interacts with *cut* during wing-margin development, as our genetic data suggest, *lola* should be expressed in wing imaginal tissue. Indeed, using a riboprobe that recognizes all variant *lola* mRNA transcripts, we found that *lola* is ubiquitously expressed throughout the wing disc (Figure 4C). Together, these results suggest that *lola* cooperates with *cut* in wing-margin development.

Overexpression of $lola^{GS}$ can rescue Cut expression and ectopically induce Wg: The overexpression data are consistent with *lola* acting genetically downstream of *cut* in wing-margin patterning, but do not rule out the possibility that *lola* suppresses the wing phenotype by restoring Cut expression in the wing discs of *cut* regulatory mutants. To determine if the $lola^{GS}$ line rescues Cut expression, we examined the pattern of Cut protein in ct^{53d} wing imaginal discs in either the presence or the absence of driving $lola^{GS[A916]}$ in the wing margin. In ct^{53d} mutant discs, Cut expression is reduced throughout the wing margin and completely absent at the presumptive wing tip, corresponding to the region of the adult wing most visibly disrupted (Figure 4, D and E). Overexpression of $lola^{GS[A916]}$ in the wing margin rescues Cut expression in ct^{53d} mutants (Figure 4F), indicating that *lola* may be involved in regulating Cut expression.

Although *C96-Gal4*-driven expression at the presumptive margin is broader than the normal Cut expression domain (Figure 4A), ectopic Cut is not observed outside of the margin cells in response to $lola^{GS[916]}$. Similarly, when $lola^{GS[A916]}$ was overexpressed along the anterior/posterior boundary using the *patched-Gal4* driver (*ptc-Gal4*; Figure 4G), ectopic Cut expression was not observed (data not shown). In contrast, *ptc-Gal4*-directed $lola^{GS[A916]}$ overexpression resulted in ectopic Wg protein in cells immediately adjacent to the dorsoventral boundary (Figure 4, G–I). Although $lola^{GS[A916]}$ can be active in wing-blade cells, as shown by ectopic Wg expression, rescued Cut expression remains confined to the margin cells, suggesting that some unknown factor, other than Lola, is involved in restricting Cut expression to margin cells.

These results suggested that *lola* may be required for wild-type wing-margin morphogenesis. To test this, we generated somatic clones of *lola* mutant cells using the FLP/FRT method (XU and RUBIN 1993). In homozygous *lola* mutant clones located adjacent to or bisecting the wing margin, neither Cut expression nor the morphology of wing-margin bristles is disrupted (data not shown). Thus, it appears that *lola*, although sufficient to rescue decreased levels of Cut expression, is not absolutely required for Cut expression and margin development of otherwise wild-type wing discs, but strongly influences the development of wings with compromised *cut* activity.

Disruption of Brahma complex activity suppresses the ct^K phenotype: Among the GS lines able to completely rescue the ct^K phenotype, we identified a GS vector insertion in the first exon of *mor* (designated $mor^{GS[A897]}$; Figure 5, A and B, and Table 3). On the basis of its failure to complement the lethality of hypomorphic mor^1 mutants, $mor^{GS\ [A897]}$ behaves genetically like a loss-of-func-

TABLE 3

Summary of the genetic interactions between Brahma complex genes and *cut* alleles

Drosophila BRM complex gene	Yeast homolog	Allele/deficency/ transgenic	Penetrance of ct^K phenotype[a]	*n* (%)	Penetrance of ct^{53d} phenotype[b]	*n* (%)
negative control		*w*		1380 (99)		704 (58)
		UAS-lacZ		1108 (99)		ND
brm	*SWI2/SNF2*	*brm[2]*	−/+	192 (100)	++	240 (88)
		Df(3L)brm11	−/+	94 (99)	+++	180 (100)
		UAS-brm[K804R]	—	176 (62)	+++	64 (100)
mor	*SWI3*	*mor[1]*	—	152 (46)	++	248 (88)
		mor[GSA897]	—	120 (18)	++	146 (88)
		Df(3R)Exel7327	−/+	192 (98)	++	168 (87)
SNF5-related 1(*Snr1*)	*SNF5*	*Snr1[01319]*	−/+	192 (100)	−/+	254 (60)
BAP111[c]	High-mobility group (HMG)-like protein	*Df(1)18.1.15*	−/+			ND
BAP60[c]	*SWP73/RSC6*	*Df(1)N12*	−/+		−/+	
BAP55	Actin-related protein	*Df(2R)Exel7147*	−/+	168 (100)	−/+	144 (65)
		BAP complex				
Osa	*SWI1*	*Osa[2]*	−/+	298 (100)	−/+	286 (67)
		UAS-osa[s2]	−/+	194 (100)	—	46 (0)
		UAS-osa[AD]	−/+	204 (100)	+++	160 (98)
		UAS-osa[RD]	−/+	422 (98)	—	284 (0)
		PBAP complex genes				
Polybromo	*Rsc1, Rsc2, Rsc4*	*Df(3R)slo8*	−/+	56 (100)	+++	110 (100)
BAP170		*Df(2R)ED1552*	−/+	146 (100)	+++	116 (91)

Results from genetic interaction studies are summarized: *n*, the total number of wings scored; ND, not determined; −/+, no effect; − and +, the degree to which the penetrance of the *cut* wing phenotype in the anterior wing margin was suppressed and enhanced, respectively.

[a] The wings of the genotype ct^K/Y; *[specified BRM complex gene]/C96-Gal4* were scored for suppression of anterior margin bristle loss. The penetrance of the ct^K wing phenotype is given as a percentage of total wings displaying gaps in the anterior wing margin sensory bristles. Note that the negative control experiments (*w* and *UAS-lacZ*) display a completely penetrant ct^K wing phenotype (~99%).

[b] The wings of the genotype $ct5^{3d}/Y$; *[specified BRM complex gene]/C96-Gal4* were scored for either the suppression or the enhancement of the ct^{53d} wing phenotype. Note that the negative control experiment (*w*) displays an incompletely penetrant ct^{53d} wing phenotype (~58%).

[c] *BAP111* and *BAP60* were recombined onto both ct^K and ct^{53d} X chromoxomes. The phenotype of females heterozygous for the respective deficiencies and homozygous for the *cut* mutations was compared to females homozygous for the *cut* mutations only.

tion allele (data not shown). In addition, $mor^{GS[A897]}$ suppressed ct^K independently of the presence of the *C96-Gal4* driver. To determine if a reduction of *mor* function is indeed responsible for suppression, we tested the ability of mor^1 to interact with ct^K. Adult males of the genotype ct^K/Y; $mor^1/+$ display a near-complete restoration of anterior wing-margin structures normally disrupted or missing in ct^K mutants, including L1 wing-vein tissue and triple-row sensory bristles (Figure 5C and Table 3). Surprisingly, the deficiencies *Df(3R)sbd105* (deficiency suppressor screen) and *Df(3R)Exel7327* (Table 3), both covering the *mor* locus, only weakly suppress the severity of the ct^K phenotype. It is not clear why the hypomorphic *mor* alleles suppress ct^K more strongly than a *mor* deficiency does. Perhaps the *cut* wing phenotype is particularly sensitive to the level of Mor activity, or the deficiencies have accumulated modifier mutations that are not present in *mor* hypomorphs, which act to conceal the suppressive effect of reduced Mor function.

mor encodes a core component of the Drosophila SWI/SNF-related ATP-dependent chromatin remodeling complex, the BRM complex (Crosby *et al.* 1999). The BRM complex is a multimeric complex containing the core catalytic subunit encoded by *brm*, and it governs an epigenetic mechanism through which the restructuring of nucleosomal DNA establishes and maintains patterns of gene expression (or repression) during development (for review, see Becker and Horz 2002). To determine if loss-of-function *mor* mutations suppressed ct^K via a reduction in BRM complex activity, several *brm* alleles were tested for the ability to interact with ct^K in the wing margin. Contrary to *mor* mutations, both the amorphic brm^2 allele (Kennison and Tamkun 1988) and the *brm* deficiency, *Df(3L)brm11*, failed to suppress the ct^K phenotype (Table 3). Perhaps the level of Mor protein is limiting with regard to Brm activity and the suppression of the ct^K phenotype.

To reduce Brm activity further, a dominant-negative

brm transgene, *UAS-brm*^{K804R} (Elfring *et al.* 1998), was overexpressed specifically in the presumptive wing margin, using the *C96-Gal4* driver. The Brm^{K804R} protein is defective in its ability to hydrolyze ATP, but maintains an association with other BRM complex components. Brm^{K804R} strongly suppresses the *ct*^{K}-dependent loss of margin sensory bristles (Figure 5D and Table 3), suggesting that reducing energy-dependent BRM complex activity, without disrupting the interactions among components of the complex *per se*, suppresses the *ct*^{K} wing-margin phenotype. Thus, manipulating the activity of the BRM complex components Mor and Brm strongly modifies *ct*^{K}-dependent wing-margin loss.

Disruption of Brahma complex activity enhances the *ct*^{53d} phenotype: The gypsy retrotransposon inserted 5′ to the *cut* coding region in *ct*^{K} disrupts communication between the distal *cut* wing enhancer and the proximal core promoter (Jack *et al.* 1991), possibly by affecting higher-order chromatin structure (Chen and Corces 2001; Byrd and Corces 2003). To determine if the disruption of BRM complex activity suppresses the *ct*^{K} wing-margin phenotype via a gypsy-dependent or -independent mechanism, we examined the genetic interactions of *mor* and *brm* mutants with other gypsy and non-gypsy *cut* alleles. We find that both *mor*^{1} and *brm*^{2} heterozygote mutations interact with the non-gypsy *ct*^{53d} allele. In contrast to the interaction with *ct*^{K}, however, we observed aggravation rather than suppression of the *ct*^{53d} phenotype (Table 3). Similarly, wing-margin-specific overexpression of Brm^{K804R} severely enhanced the loss of anterior margin tissue in *ct*^{53d} (Figure 5, E and F). The loss of wing-margin bristles observed in *ct*^{K} and *ct*^{53d} mutants likely reflects a decrease in Cut expression in the wing margin (Figure 6A). Cut expression is substantially restored in *ct*^{K}*/Y;UAS-brm*^{K804R}*/C96-Gal4* wing imaginal discs (data not shown). Conversely, the aggravated loss of wing-margin bristles of *ct*^{53d}*/Y;UAS-brm*^{K804R}*/C96-Gal4* correlates with a further decrease in the level of Cut protein throughout the presumptive wing margin in *ct*^{53d} mutant discs (Figure 6B).

Differences in the nature of the genetic aberrations associated with the *cut* wing enhancer region may account for the apparent discrepancy in the suppression *vs.* the enhancement of the wing phenotypes observed in response to disruptions of BRM complex activity. Neither heterozygous *mor*^{1} or *brm*^{2} mutations nor the overexpression of UAS-Brm^{K804R} modifies the phenotype of the strong *cut* wing alleles, *ct*^{6} (gypsy) or *ct*^{2s} (non-gypsy) (data not shown). It is conceivable that Cut expression in *ct*^{6} and *ct*^{2s} mutants is reduced to a level beyond which a reduction in BRM complex activity can no longer produce an effect on wing-margin development. In any case, the preceding results demonstrate that the BRM complex contributes to both gypsy-dependent and gypsy-independent regulation of Cut expression in the wing margin (see discussion).

Both BAP and PBAP interact with *cut*: In Drosophila, there are two distinct Brm-containing complexes, BAP (Brahma-associated proteins) and PBAP (Polybromo-associated BAP). Both complexes contain the DNA-dependent ATPase Brm and seven core subunits, Mor/BAP155, BAP111, BAP74 (hsp70 cognate hsc4), BAP60, BAP55, actin/BAP47, and Snr1/BAP45 (Mohrmann *et al.* 2004). Heterozygous loss-of-function mutations in *BAP111*, *BAP60*, *BAP55*, or *Snr1/BAP45* did not modify the *ct*^{K} or *ct*^{53d} margin bristle phenotype (Table 3), suggesting that decreasing the expression level of these subunits is not limiting for BRM complex activity *in vivo*.

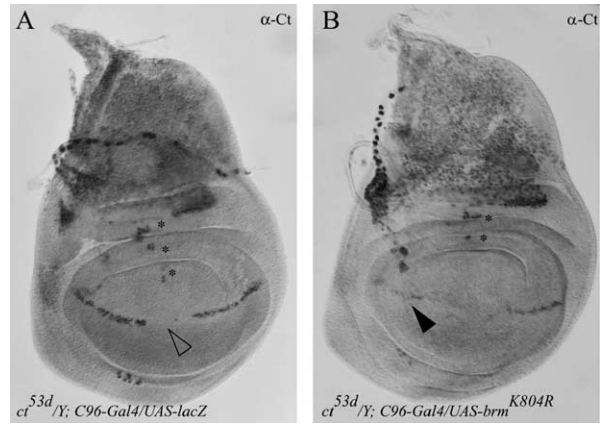

Figure 6.—The expression of Cut is reduced in response to the disruption of the Brahma complex. (A) In *ct*^{53d} mutants, Cut expression is reduced at the presumptive wing tip (open arrowhead). (B) Overexpression of a dominant-negative form of Brm further reduces the level of Cut expression in *ct*^{53d} mutants (solid arrowhead). Note that Cut is still expressed in some sensory precursor cells outside of the *C96-Gal4* expression domain (asterisks).

The BAP and PBAP complexes are distinguished by association with either Osa or Polybromo and BAP170, respectively (Mohrmann *et al.* 2004). Thus, we examined the ability of *osa*, *polybromo*, and *BAP170* loss-of-function mutations to enhance the *ct*^{53d} wing phenotype. Flies heterozygous for the *osa*^{2} allele do not display wing defects alone, nor does *osa*^{2} cause a strong enhancement of the *ct*^{53d} phenotype. However, the overexpression of the full-length *UAS-osa* transgene (Collins *et al.* 1999) specifically in the wing margin suppressed the loss of anterior margin bristles of the *ct*^{53d} phenotype (Table 3), implying that an Osa-associated BRM complex interacts with *cut* during margin development by increasing its activity.

Specific mutations are not available for either *polybromo* or *BAP170*. Therefore, we used the deficiencies *Df(3R)slo8* and *Df(2R)ED1552*, covering *polybromo* and *BAP170*, respectively, to explore the genetic interaction with *ct*^{53d}. As with *brm* or *mor* mutations, both deficiencies enhanced margin bristle and tissue loss of *ct*^{53d} (Table 3). Although it cannot be ruled out that one of the other genes disrupted by the deficiencies is responsible for the enhancement of the *ct*^{53d} phenotype, these data support the idea that *cut* activity is sensitive to disruptions of PBAP complex components. It should be noted

that neither *osa* mutations nor the *polybromo* or *BAP170* deficiencies were able to modify the phenotype of ct^{K}. Overall, the genetic data suggest that both Brm-containing chromatin-remodeling complexes, BAP and PBAP, may contribute to *cut*-dependent wing-margin development in a complex manner.

Osa may act as a transcriptional repressor in its interaction with ct^{53d}: An Osa-containing BRM complex has previously been implicated in the repression of Wg target genes during development of the wing imaginal disc (Collins and Treisman 2000). To study whether Osa acts as a transcriptional activator or repressor with regard to its interaction with *cut*, we examined the ability of obligatory activator and repressor forms of Osa (Collins *et al.* 1999) to modify the ct^{53d} phenotype (Table 3). Wing-margin-specific overexpression of the Osa AT-rich interaction domain (ARID)-DNA-binding domain fused to the Engrailed repression domain ($UAS\text{-}Osa^{RD[11c]}$) strongly suppressed the ct^{53d} phenotype, but had no effect in a wild-type background. As previously stated, overexpression of full-length Osa also ameliorates the ct^{53d} phenotype, consistent with the idea that Osa acts as a repressor. Conversely, overexpression of the Osa-ARID domain fused to the VP16 transcriptional activation domain ($UAS\text{-}Osa^{AD[20e]}$) enhanced the wing-margin phenotype of ct^{53d}. Together, these results suggest that the Osa-containing BAP complex must act as a transcriptional repressor to ameliorate *cut*-dependent wing-margin patterning defects. This is in accordance with the repressive activity of Osa on Wg target genes in the wing disc (Collins and Treisman 2000).

DISCUSSION

The identity of genes that interact with *cut* during wing-margin patterning: Does Cut regulate cell growth and proliferation? The secreted morphogen encoded by *wg* patterns the wing margin by coordinating cell growth and proliferation with cell differentiation (Phillips and Whittle 1993; Johnston and Edgar 1998; Nepveu 2001; Duman-Scheel *et al.* 2004). Additionally, Wg is required for the survival of margin cells (Johnston and Sanders 2003). Expression of Wg within the presumptive wing margin is maintained by Cut, and in the absence of Cut the wing margin degenerates (Jack *et al.* 1991). Here, we determined that wing-margin development requires *cut* activity independently of the maintenance of Wg expression. Inhibiting wing-margin degeneration without rescuing margin bristle development in *cut* mutants by supplying exogenous Wg expression or the apoptosis inhibitor p35 demonstrates a requirement for Cut in margin sensory organ development, which is separable from its role in maintaining Wg expression. Although Wg is not sufficient for margin bristle formation in the absence of *cut*, it remains to be determined if transduction of the Wg signal is required cell autonomously within the Cut-positive margin cells for margin sensory organ development. Indeed, expression of the proneural gene *achaete* in bristle progenitors along the anterior margin depends upon canonical Wg signaling (Phillips and Whittle 1993).

As a means to further elucidate the role of *cut* in wing-margin patterning, we performed complementary loss- and gain-of-function genetic screens to identify other genes that modify the *cut* wing phenotype. Several classes of *cut* modifiers include loci near known genes that regulate processes influencing cell growth and proliferation, including *brat*, *CycE*, *eIF4A*, and *eIF4E*. The identification of these genes suggests that during wing-margin development Cut activity may be regulated in a manner dependent upon cell cycle phasing and/or may coordinate cell cycle progression with terminal specification of cell identity. This is consistent with the proposed activity of the vertebrate Cut homolog CDP/Cux1, the DNA-binding activity of which is modulated in coordination with cell cycle progression and is postulated to synchronize cell cycle exit with terminal cell differentiation (reviewed in Nepveu 2001)

***lola* is required in the context of decreased Cut expression for wing-margin development:** *lola* is known for its role as a regulator of axon growth in Drosophila and is proposed to coordinately control the expression of multiple genes that execute axon guidance decisions (Giniger *et al.* 1994; Madden *et al.* 1999; Crowner *et al.* 2002). We identified a novel role for *lola* in wing-margin development, revealed by its gain- and loss-of-function genetic interactions with hypomorphic *cut* alleles. Overexpression directed by $lola^{GS}$ insertions is sufficient to rescue the reduction in Cut expression of regulatory *cut* mutants and to suppress the hypoplastic *cut* wing phenotype. Conversely, loss of *lola* function aggravates the *cut* wing-margin defects. It is feasible that Lola modulates Cut expression by interacting directly or indirectly with the *cut* wing-margin enhancer or with other regulatory regions adjacent to or distant from this enhancer, which may also be involved in promoting Cut expression at the margin. The suppression of the *cut* wing phenotype by Lola misexpression is consistent with other alternative possibilities, such as that Lola may be involved in the regulation of an unknown Cut target gene, may be a Cut target itself, or both. Consistent with the ability to interact with *cut* during wing development, *lola* mRNA is expressed ubiquitously in the imaginal wing disc. However, the requirement for *lola* in wing development is evident only in *cut* mutants, since in *lola* null mutant cell clones Cut expression and wing-margin development is not disrupted. It may be that *lola* plays a nonessential role in the regulation of processes directing wing-margin development, which only becomes apparent when Cut activity is decreased, akin to the cryptic variations necessary for evolutionary adaptations (Gibson and Dworkin 2004).

Overexpression of Lola in *cut* mutants suppresses the margin loss phenotype presumed to result from a failure

to maintain expression of the secreted factor Wg at the dorsal/ventral boundary of the wing disc. We demonstrate that Lola induces ectopic Wg expression at locations proximal to the dorsal/ventral boundary. Thus, it may be that Lola overexpression rescues wing-blade tissue in *cut* mutants via the induction of Wg expression. The suppression of sensory bristle loss, however, is likely independent of this effect on Wg expression. It will be interesting to determine if *lola* contributes to other tissue-specific aspects of *cut* activity.

The induction and refinement of both Wg and Cut expression at the wing dorsal/ventral boundary requires activation of the Notch signaling pathway (Diaz-Benjumea and Cohen 1995; Micchelli *et al.* 1997). The induction of Cut and Wg expression in response to Lola overexpression implies that Lola may positively regulate Notch signaling in wing boundary cells. In the eye, however, Lola appears to act in the converse manner, where the loss of Lola function enhances the rough-eye phenotype resulting from the overexpression of a constitutively active form of Notch (Verheyen *et al.* 1996). Clonal analysis of amorphic *lola* mutations does not produce the incised wing-margin phenotype indicative of a loss of Notch function, suggesting that Lola activity is not required to regulate Notch signaling. Furthermore, although Cut expression is rescued in the wing-margin in response to broad Lola overexpression, it is not expanded outside of the boundary cells. This is in contrast to the observed expansion of Wg into cells adjacent to the boundary, indicating that the induction of Wg is independent of Cut. Since ectopic expression of both Wg and Cut is induced in the wing disc in response to activated Notch (de Celis *et al.* 1996), expanded Wg expression due to Lola overexpression may not involve Notch signaling.

The *lola* locus encodes a family of at least 20 BTB-zinc-finger transcription factors, expressed in partially distinct tissue-specific patterns. The functional significance of the diversity in Lola isoforms and their expression patterns is not entirely clear. In several instances, mutations inactivating a single Lola isoform affect only a subset of axon guidance defects associated with amorphic *lola* alleles (Goeke *et al.* 2003). This led to the hypothesis that specific isoforms and interactions with cofactors contribute to the diversity in *lola*-dependent axon guidance decisions. Lola isoform F has been shown to physically interact *in vitro* with the chromosomal JIL-1 kinase (Zhang *et al.* 2003). JIL-1 regulates chromatin structure by influencing the phosphorylation state of histone 3 (Wang *et al.* 2001). Amorphic *lola* alleles act as dominant modifiers of a hypomorphic JIL-1 allele, leading to an increase in embryonic viability (Zhang *et al.* 2003). It is not clear, however, if Lola isoform F is responsible for the *in vivo* genetic interaction with JIL-1. Similarly, we were unable to determine which Lola isoform(s) is responsible for the interaction with *cut* in the wing margin. All amorphic *lola* alleles interact with *cut* (*i.e.*, enhancement of bristle loss) in a similar manner. Interestingly, the axon guidance decision-selective $lola^{ORE119}$ allele, thought to disrupt only isoform L, enhanced the *cut* wing phenotype, whereas the isoform K-specific $lola^{ORC4}$ allele did not.

Brm-associated chromatin-remodeling complexes regulate multiple aspects of wing development: In Drosophila, Brm and Brm-associated proteins regulate multiple aspects of wing development. Early in wing development, Brm and Osa modulate the activity of the dorsal wing compartment specific selector gene, *Apterous*, and the subsequent localization of the Wg-dependent organizer at the dorsal/ventral boundary (Milan *et al.* 2004). Similarly, Mor is required for the expression of the posterior compartment specific selector gene *engrailed* (Brizuela and Kennison 1997). The triune of Brm, Osa, and Mor is required to repress the Wg target gene *nubbin*, a gene required for the growth and patterning of the wing (Collins and Treisman 2000). Finally, Brm activity is required for the cell-type-specific activation and repression of genes involved in wing-vein elaboration (Marenda *et al.* 2004). Our genetic analysis indicates that *cut*-dependent wing-margin patterning also relies upon the activity of Brm, as well as upon the activity of several Brm-associated subunits of both the BAP and the PBAP complex. Heterozygous loss-of-function mutations in the core subunits Brm and Mor, although individually having no effect on normal wing-margin development, enhance the loss of wing-margin tissue of the ct^{53d} allele. Deficiencies covering the PBAP subunits, BAP170 and Polybromo, or the overexpression of BAP subunit Osa, exhibit similar interactions with ct^{53d}. The enhancement of the ct^{53d} wing phenotype correlates with a decrease in Cut expression in the presumptive wing margin, thus indicating that the BRM complex activity is required genetically upstream of *cut*. Together with other studies, our data support the idea that the BRM complex may globally regulate the expression of genes required for wing development.

How might the BRM complex regulate *cut* expression in the wing? The regulation of the distal *cut* wing enhancer requires the activity of both enhancer-binding and enhancer-facilitator proteins. Enhancer-facilitator proteins are proposed to structurally facilitate communication between distal enhancer elements and the proximal promoter and are different from enhancer-binding (co)activators in that they do not directly activate the initiation of transcription. A number of genes, including *scalloped* (*sd*), *mastermind* (*mam*), *Chip* (*Chi*), and *Nipped-B*, are involved in the regulation of *cut* expression (Morcillo *et al.* 1996; Rollins *et al.* 1999). Genetic and biochemical data suggest that *sd* and *mam* encode *cut* wing-margin enhancer-binding transcriptional (co)activators. Consistent with their role as enhancer-binding activator proteins, loss-of-function *sd* and *mam* mutations enhance the severity of the *cut* wing phenotype resulting from deletions in the wing en-

hancer. In contrast, *Chip* and *Nipped-B* encode putative general enhancer-facilitator proteins (Morcillo *et al.* 1996, 1997; Rollins *et al.* 1999, 2004) and primarily enhance the *cut* wing phenotype of *cut* alleles in which enhancer-promoter communication is partially compromised by the gypsy insulator.

Given the known regulatory mechanisms imposed upon *cut* expression and the recognized ability of the BRM complex to affect chromatin structure, several mechanisms can be envisioned through which the BRM complex may directly or indirectly regulate *cut* expression in the wing margin. The BRM complex may indirectly influence *cut* expression via the expression of *cut* wing enhancer-binding or enhancer-facilitating proteins. Alternatively, the BRM complex may regulate the local chromatin structure of 5′ *cut* regulatory regions and affect the access of enhancer-binding proteins and/or the basal transcriptional machinery to DNA. Our data do not distinguish between these possibilities. Similar to *sd* and *mam*, both *brm* and *mor* display a strong genetic interaction with the ct^{53d} wing-margin enhancer deletion. Furthermore, the overexpression of a dominant negative form of Brm dramatically reduced Cut expression throughout the entire wing margin in the ct^{53d} mutant background, but had a less pronounced effect in a wild-type background. Thus, Cut expression is particularly sensitive to disruptions in BRM complex activity when the wing-margin enhancer is partially inactivated by deletions. Therefore, it is possible that the BRM complex normally acts to positively regulate *cut* expression through a direct or indirect interaction with enhancer-binding proteins, such as Sd or Mam. However, it is also possible that alterations in chromatin structure may be essential for the remote *cut* wing enhancer to interact with the proximal promoter. Consistent with this possibility, the BRM complex component Osa physically interacts with the enhancer-facilitator Chip (Heitzler *et al.* 2003). Similarly, Nipped-B interacts with the Drosophila cohesin complex, a negative regulator of the *cut* wing enhancer (Rollins *et al.* 2004). The interaction of the human cohesin complex with chromatin requires hISWI chromatin-remodeling complex activity (Hakimi *et al.* 2002). Although the nature of the interaction of these factors with the *cut* enhancer region remains to be determined, our data indicate that enhancer/promoter communication requires BRM complex chromatin-remodeling activity. In addition to mediating *cut* enhancer activity, BRM complex activity also seems to be required for gypsy-mediated insulation. Thus the BRM complex and other group B candidates may contribute to the regulation of transcription at multiple levels.

Alternatively, the BRM complex may interact with the autoregulation of *cut* expression. In the embryonic peripheral nervous system, ectopic Cut expression activates the endogenous *cut* locus. Autoregulatory maintenance of Cut expression appears to be essential for sensory organ development (Blochlinger *et al.* 1991), and it is possible that the BRM complex activity may assist in this process. Accordingly, subthreshold levels of *cut* activation in the wing margin, below that required for the maintenance of its own expression, may affect the stochastic, cell-autonomous loss of sensory bristles along the anterior wing margin.

Is the BRM complex required for gypsy insulation activity? Regulatory lesions affecting the activity of the *cut* wing-margin enhancer are responsive to disruptions of Brm activity. The differential effects of disrupting either Brm or Mor activity on the ct^{K} and ct^{53d} wing phenotypes possibly reflect differences in the nature of these regulatory lesions (*i.e.*, gypsy insertion or partial wing enhancer deletion). In contrast to the ct^{53d} allele interaction, disruptions in BRM complex activity suppressed the discontinuities in the wing bristles of the gypsy ct^{K} allele. The gypsy insulator disrupts communication between the distal *cut* wing enhancer and the proximal promoter. *Su(Hw)*] and *mod(mdg4)* are required for gypsy activity and are postulated to do so by directly interfering with the enhancer-facilitator activity of Chip (Gause *et al.* 2001). Loss-of-function mutations in either gene suppress the *cut* wing phenotype resulting from gypsy.

Several lines of evidence suggest that the regulation of higher-order chromatin structure is involved in the control of gypsy activity. First, in diploid cells, Su(Hw) and Mod(mdg4) colocalize with gypsy and other native insulating elements at peri-nuclear locations (Gerasimova and Corces 1998). These sites represent clustering of distant insulator elements. The subnuclear localization of gypsy and its regulatory proteins is suggestive of a higher-order chromatin structure. In *Su(Hw)* mutants, mod(mdg4) protein and gypsy insulator sequences fail to cluster at peri-nuclear sites and are instead diffusely distributed in the nucleus. The peri-nuclear localization of gyspy, however, does not appear to be required for insulator activity (Xu *et al.* 2004). Second, *mod(mdg4)* interacts genetically with several *trithorax group* (*trxG*) genes, known regulators of homeotic gene expression (Buchner *et al.* 2000). *trxG* genes, including *mor* and *brm*, affect the post-translational modification of histone proteins, influencing nucleosome organization and chromatin structure. Therefore, Mod(mdg4) may influence chromatin structure within the confine of gypsy-mediated insulation through an interaction with *trxG* genes. Finally, mutations in several *trxG* genes disrupt the peri-nuclear location of Su(Hw)/mod(mdg4)/gypsy complexes, a phenotype resembling *Su(Hw)* mutations (Gerasimova and Corces 1998). It has been suggested that a general mechanism influencing higher-order chromatin structure may be involved in both regulation of gypsy activity and homeotic gene expression. Consistent with the activity of other *trxG* genes, we propose that wild-type BRM complex activity is required for the productive interaction between Su(Hw) and the gypsy insulator. The absence or the reduction of BRM com-

plex activity would preclude gypsy insulation and thus restore normal levels of Cut expression.

We thank D. Dorsett, E. Giniger, J. Treisman, T. Aigaki, and the Bloomington Stock Center for providing fly stocks. We also thank D. Dorsett and J. Treisman for comments on the manuscript. J.J.K. was supported by a fellowship from the Hearing and Chemical Senses training grant (National Institutes of Health/National Institute on Deafness and Other Communication Disorders 5 T32 DC00011).

LITERATURE CITED

Andres, V., M. D. Chiara and V. Mahdavi, 1994 A new bipartite DNA-binding domain: cooperative interaction between the cut repeat and homeo domain of the cut homeo proteins. Genes Dev. **8:** 245–257.

Becker, P. B., and W. Horz, 2002 ATP-dependent nucleosome remodeling. Annu. Rev. Biochem. **71:** 247–273.

Blochlinger, K., R. Bodmer, J. Jack, L. Y. Jan and Y. N. Jan, 1988 Primary structure and expression of a product from cut, a locus involved in specifying sensory organ identity in Drosophila. Nature **333:** 629–635.

Blochlinger, K., R. Bodmer, L. Y. Jan and Y. N. Jan, 1990 Patterns of expression of cut, a protein required for external sensory organ development in wild-type and cut mutant Drosophila embryos. Genes Dev. **4:** 1322–1331.

Blochlinger, K., L. Y. Jan and Y. N. Jan, 1991 Transformation of sensory organ identity by ectopic expression of Cut in Drosophila. Genes Dev. **5:** 1124–1135.

Bodmer, R., S. Barbel, S. Sheperd, J. W. Jack, L. Y. Jan *et al.*, 1987 Transformation of sensory organs by mutations of the cut locus of D. melanogaster. Cell **51:** 293–307.

Brizuela, B. J., and J. A. Kennison, 1997 The Drosophila homeotic gene moira regulates expression of engrailed and HOM genes in imaginal tissues. Mech. Dev. **65:** 209–220.

Buchner, K., P. Roth, G. Schotta, V. Krauss, H. Saumweber *et al.*, 2000 Genetic and molecular complexity of the position effect variegation modifier *mod*(*mdg4*) in Drosophila. Genetics **155:** 141–157.

Byrd, K., and V. G. Corces, 2003 Visualization of chromatin domains created by the gypsy insulator of Drosophila. J. Cell Biol. **162:** 565–574.

Chen, S., and V. G. Corces, 2001 The gypsy insulator of Drosophila affects chromatin structure in a directional manner. Genetics **159:** 1649–1658.

Collins, R. T., and J. E. Treisman, 2000 Osa-containing Brahma chromatin remodeling complexes are required for the repression of wingless target genes. Genes Dev. **14:** 3140–3152.

Collins, R. T., T. Furukawa, N. Tanese and J. E. Treisman, 1999 Osa associates with the Brahma chromatin remodeling complex and promotes the activation of some target genes. EMBO J. **18:** 7029–7040.

Coqueret, O., G. Berube and A. Nepveu, 1998 The mammalian Cut homeodomain protein functions as a cell-cycle-dependent transcriptional repressor which downmodulates p21WAF1/CIP1/SDI1 in S phase. EMBO J. **17:** 4680–4694.

Crosby, M. A., C. Miller, T. Alon, K. L. Watson, C. P. Verrijzer *et al.*, 1999 The trithorax group gene moira encodes a brahma-associated putative chromatin-remodeling factor in Drosophila melanogaster. Mol. Cell. Biol. **19:** 1159–1170.

Crowner, D., K. Madden, S. Goeke and E. Giniger, 2002 Lola regulates midline crossing of CNS axons in Drosophila. Development **129:** 1317–1325.

Dansereau, D. A., M. D. Lunke, A. Finkielsztein, M. A. Russell and W. J. Brook, 2002 Hephaestus encodes a polypyrimidine tract binding protein that regulates Notch signalling during wing development in Drosophila melanogaster. Development **129:** 5553–5566.

de Celis, J. F., A. Garcia-Bellido and S. J. Bray, 1996 Activation and function of Notch at the dorsal-ventral boundary of the wing imaginal disc. Development **122:** 359–369.

Diaz-Benjumea, F. J., and S. M. Cohen, 1995 Serrate signals through Notch to establish a Wingless-dependent organizer at the dorsal/ventral compartment boundary of the Drosophila wing. Development **121:** 4215–4225.

Dorsett, D., 1993 Distance-independent inactivation of an enhancer by the suppressor of Hairy-wing DNA-binding protein of Drosophila. Genetics **134:** 1135–1144.

Duman-Scheel, M., L. A. Johnston and W. Du, 2004 Repression of dMyc expression by Wingless promotes Rbf-induced G1 arrest in the presumptive Drosophila wing margin. Proc. Natl. Acad. Sci. USA **101:** 3857–3862.

Elfring, L. K., C. Daniel, O. Papoulas, R. Deuring, M. Sarte *et al.*, 1998 Genetic analysis of brahma: the Drosophila homolog of the yeast chromatin remodeling factor SWI2/SNF2. Genetics **148:** 251–265.

Ellis, T., L. Gambardella, M. Horcher, S. Tschanz, J. Capol *et al.*, 2001 The transcriptional repressor CDP (Cutl1) is essential for epithelial cell differentiation of the lung and the hair follicle. Genes Dev. **15:** 2307–2319.

Epps, J. L., and S. Tanda, 1998 The Drosophila semushi mutation blocks nuclear import of bicoid during embryogenesis. Curr. Biol. **8:** 1277–1280.

Frank, D. J., B. A. Edgar and M. B. Roth, 2002 The Drosophila melanogaster gene brain tumor negatively regulates cell growth and ribosomal RNA synthesis. Development **129:** 399–407.

Garcia-Bellido, A., 1975 Genetic control of wing disc development in Drosophila. Ciba Found. Symp., No. 29: 161–182.

Gause, M., P. Morcillo and D. Dorsett, 2001 Insulation of enhancer-promoter communication by a gypsy transposon insert in the Drosophila cut gene: cooperation between suppressor of hairy-wing and modifier of mdg4 proteins. Mol. Cell. Biol. **21:** 4807–4817.

Gebauer, F., and M. W. Hentze, 2004 Molecular mechanisms of translational control. Nat. Rev. Mol. Cell Biol. **5:** 827–835.

Gerasimova, T. I., and V. G. Corces, 1998 Polycomb and trithorax group proteins mediate the function of a chromatin insulator. Cell **92:** 511–521.

Ghosh, D., T. I. Gerasimova and V. G. Corces, 2001 Interactions between the Su(Hw) and Mod(mdg4) proteins required for gypsy insulator function. EMBO J. **20:** 2518–2527.

Gibson, G., and I. Dworkin, 2004 Uncovering cryptic genetic variation. Nat. Rev. Genet. **5:** 681–690.

Giniger, E., K. Tietje, L. Y. Jan and Y. N. Jan, 1994 lola encodes a putative transcription factor required for axon growth and guidance in Drosophila. Development **120:** 1385–1398.

Glaser, R. L., M. F. Wolfner and J. T. Lis, 1986 Spatial and temporal pattern of hsp26 expression during normal development. EMBO J. **5:** 747–754.

Goeke, S., E. A. Greene, P. K. Grant, M. A. Gates, D. Crowner *et al.*, 2003 Alternative splicing of lola generates 19 transcription factors controlling axon guidance in Drosophila. Nat. Neurosci. **6:** 917–924.

Gould, A. P., and R. A. White, 1992 Connectin, a target of homeotic gene control in Drosophila. Development **116:** 1163–1174.

Goulet, B., A. Baruch, N. S. Moon, M. Poirier, L. L. Sansregret *et al.*, 2004 A cathepsin L isoform that is devoid of a signal peptide localizes to the nucleus in S phase and processes the CDP/Cux transcription factor. Mol. Cell **14:** 207–219.

Grueber, W. B., L. Y. Jan and Y. N. Jan, 2003 Different levels of the homeodomain protein cut regulate distinct dendrite branching patterns of Drosophila multidendritic neurons. Cell **112:** 805–818.

Gupta, S., M. X. Luong, S. A. Bleuming, A. Miele, M. Luong *et al.*, 2003 Tumor suppressor pRB functions as a co-repressor of the CCAAT displacement protein (CDP/cut) to regulate cell cycle controlled histone H4 transcription. J. Cell. Physiol. **196:** 541–556.

Gustafson, K., and G. L. Boulianne, 1996 Distinct expression patterns detected within individual tissues by the GAL4 enhancer trap technique. Genome **39:** 174–182.

Hakimi, M. A., D. A. Bochar, J. A. Schmiesing, Y. Dong, O. G. Barak *et al.*, 2002 A chromatin remodelling complex that loads cohesin onto human chromosomes. Nature **418:** 994–998.

Hardiman, K. E., R. Brewster, S. M. Khan, M. Deo and R. Bodmer, 2002 The *bereft* gene, a potential target of the neural selector gene *cut*, contributes to bristle morphogenesis. Genetics **161:** 231–247.

Heitzler, P., L. Vanolst, I. Biryukova and P. Ramain, 2003 Enhancer-promoter communication mediated by Chip during Pan-

nier-driven proneural patterning is regulated by Osa. Genes Dev. **17:** 591–596.

Heuer, J. G., K. Li and T. C. Kaufman, 1995 The Drosophila homeotic target gene centrosomin (cnn) encodes a novel centrosomal protein with leucine zippers and maps to a genomic region required for midgut morphogenesis. Development **121:** 3861–3876.

Hombria, J. C., and B. Lovegrove, 2003 Beyond homeosis—HOX function in morphogenesis and organogenesis. Differentiation **71:** 461–476.

Hoover, K. K., T. I. Gerasimova, A. J. Chien and V. G. Corces, 1992 Dominant effects of *suppressor of Hairy-wing* mutations on gypsy-induced alleles of *forked* and *cut* in *Drosophila melanogaster*. Genetics **132:** 691–697.

Horiuchi, T., E. Giniger and T. Aigaki, 2003 Alternative transsplicing of constant and variable exons of a Drosophila axon guidance gene, lola. Genes Dev. **17:** 2496–2501.

Hu, N., and J. Castelli-Gair, 1999 Study of the posterior spiracles of Drosophila as a model to understand the genetic and cellular mechanisms controlling morphogenesis. Dev. Biol. **214:** 197–210.

Jack, J. W., 1985 Molecular organization of the cut locus of Drosophila melanogaster. Cell **42:** 869–876.

Jack, J., and Y. DeLotto, 1995 Structure and regulation of a complex locus: the *cut* gene of Drosophila. Genetics **139:** 1689–1700.

Jack, J., D. Dorsett, Y. Delotto and S. Liu, 1991 Expression of the cut locus in the Drosophila wing margin is required for cell type specification and is regulated by a distant enhancer. Development **113:** 735–747.

Jackson, S. M., and C. A. Berg, 1999 Soma-to-germline interactions during Drosophila oogenesis are influenced by dose-sensitive interactions between *cut* and the genes *cappuccino*, *ovarian tumor* and *agnostic*. Genetics **153:** 289–303.

Jackson, S. M., and K. Blochlinger, 1997 cut interacts with Notch and protein kinase A to regulate egg chamber formation and to maintain germline cyst integrity during Drosophila oogenesis. Development **124:** 3663–3672.

Johnston, L. A., and B. A. Edgar, 1998 Wingless and Notch regulate cell-cycle arrest in the developing Drosophila wing. Nature **394:** 82–84.

Johnston, L. A., and A. L. Sanders, 2003 Wingless promotes cell survival but constrains growth during Drosophila wing development. Nat. Cell Biol. **5:** 827–833.

Kennison, J. A., and J. W. Tamkun, 1988 Dosage-dependent modifiers of polycomb and antennapedia mutations in Drosophila. Proc. Natl. Acad. Sci. USA **85:** 8136–8140.

Khanna-Gupta, A., T. Zibello, S. Kolla, E. J. Neufeld and N. Berliner, 1997 CCAAT displacement protein (CDP/cut) recognizes a silencer element within the lactoferrin gene promoter. Blood **90:** 2784–2795.

Khanna-Gupta, A., T. Zibello, H. Sun, P. Gaines and N. Berliner, 2003 Chromatin immunoprecipitation (ChIP) studies indicate a role for CCAAT enhancer binding proteins alpha and epsilon (C/EBP alpha and C/EBP epsilon) and CDP/cut in myeloid maturation-induced lactoferrin gene expression. Blood **101:** 3460–3468.

Kim, S. Y., and G. L. Boulianne, 1998 Characterization of a novel discless mutant in *D. melanogaster*. Annu. Dros. Res. Conf. **39:** 675B.

Kremser, T., K. Hasenpusch-Theil, E. Wagner, D. Buttgereit and R. Renkawitz-Pohl, 1999 Expression of the beta3 tubulin gene (beta Tub60D) in the visceral mesoderm of Drosophila is dependent on a complex enhancer that binds Tinman and UBX. Mol. Gen. Genet. **262:** 643–658.

Lai, E. C., and V. Orgogozo, 2004 A hidden program in Drosophila peripheral neurogenesis revealed: fundamental principles underlying sensory organ diversity. Dev. Biol. **269:** 1–17.

Ledford, A. W., J. G. Brantley, G. Kemeny, T. L. Foreman, S. E. Quaggin *et al.*, 2002 Deregulated expression of the homeobox gene Cux-1 in transgenic mice results in downregulation of p27(kip1) expression during nephrogenesis, glomerular abnormalities, and multiorgan hyperplasia. Dev. Biol. **245:** 157–171.

Lewis, S. E., S. M. Searle, N. Harris, M. Gibson, V. Lyer *et al.*, 2002 Apollo: a sequence annotation editor. Genome Biol. **3:** RESEARCH0082.

Lievens, P. M., J. J. Donady, C. Tufarelli and E. J. Neufeld, 1995 Repressor activity of CCAAT displacement protein in HL-60 myeloid leukemia cells. J. Biol. Chem. **270:** 12745–12750.

Liu, S., and J. Jack, 1992 Regulatory interactions and role in cell type specification of the Malpighian tubules by the cut, Kruppel, and caudal genes of Drosophila. Dev. Biol. **150:** 133–143.

Liu, S., E. McLeod and J. Jack, 1991 Four distinct regulatory regions of the cut locus and their effect on cell type specification in Drosophila. Genetics **127:** 151–159.

Lohmann, I., N. McGinnis, M. Bodmer and W. McGinnis, 2002 The Drosophila Hox gene deformed sculpts head morphology via direct regulation of the apoptosis activator reaper. Cell **110:** 457–466.

Ludlow, C., R. Choy and K. Blochlinger, 1996 Functional analysis of Drosophila and mammalian cut proteins in files. Dev. Biol. **178:** 149–159.

Luong, M. X., C. M. van der Meijden, D. Xing, R. Hesselton, E. S. Monuki *et al.*, 2002 Genetic ablation of the CDP/Cux protein C terminus results in hair cycle defects and reduced male fertility. Mol. Cell. Biol. **22:** 1424–1437.

Madden, K., D. Crowner and E. Giniger, 1999 LOLA has the properties of a master regulator of axon-target interaction for SNb motor axons of Drosophila. Dev. Biol. **213:** 301–313.

Mann, R. S., and S. B. Carroll, 2002 Molecular mechanisms of selector gene function and evolution. Curr. Opin. Genet. Dev. **12:** 592–600.

Marenda, D. R., C. B. Zraly and A. K. Dingwall, 2004 The Drosophila Brahma (SWI/SNF) chromatin remodeling complex exhibits cell-type specific activation and repression functions. Dev. Biol. **267:** 279–293.

Merritt, D. J., 1997 Transformation of external sensilla to chordotonal sensilla in the cut mutant of Drosophila assessed by single-cell marking in the embryo and larva. Microsc. Res. Tech. **39:** 492–505.

Micchelli, C. A., E. J. Rulifson and S. S. Blair, 1997 The function and regulation of cut expression on the wing margin of Drosophila: Notch, Wingless and a dominant negative role for Delta and Serrate. Development **124:** 1485–1495.

Milan, M., T. T. Pham and S. M. Cohen, 2004 Osa modulates the expression of Apterous target genes in the Drosophila wing. Mech. Dev. **121:** 491–497.

Miron, M., P. Lasko and N. Sonenberg, 2003 Signaling from Akt to FRAP/TOR targets both 4E-BP and S6K in Drosophila melanogaster. Mol. Cell. Biol. **23:** 9117–9126.

Mogila, V. A., A. B. Ladvishenko, O. B. Simonova and T. I. Gerasimova, 1992 Intragenic suppression: Stalker, a retrovirus-like transposable element, can compensate for a deficiency at the cut locus of Drosophila melanogaster. Genetica **86:** 305–311.

Mohrmann, L., K. Langenberg, J. Krijgsveld, A. J. Kal, A. J. Heck *et al.*, 2004 Differential targeting of two distinct SWI/SNF-related Drosophila chromatin-remodeling complexes. Mol. Cell. Biol. **24:** 3077–3088.

Moon, N. S., G. Berube and A. Nepveu, 2000 CCAAT displacement activity involves CUT repeats 1 and 2, not the CUT homeodomain. J. Biol. Chem. **275:** 31325–31334.

Moon, N. S., P. Premdas, M. Truscott, L. Leduy, G. Berube *et al.*, 2001 S phase-specific proteolytic cleavage is required to activate stable DNA binding by the CDP/Cut homeodomain protein. Mol. Cell. Biol. **21:** 6332–6345.

Morcillo, P., C. Rosen and D. Dorsett, 1996 Genes regulating the remote wing margin enhancer in the Drosophila cut locus. Genetics **144:** 1143–1154.

Morcillo, P., C. Rosen, M. K. Baylies and D. Dorsett, 1997 Chip, a widely expressed chromosomal protein required for segmentation and activity of a remote wing margin enhancer in Drosophila. Genes Dev. **11:** 2729–2740.

Nepveu, A., 2001 Role of the multifunctional CDP/Cut/Cux homeodomain transcription factor in regulating differentiation, cell growth and development. Gene **270:** 1–15.

Neufeld, E. J., D. G. Skalnik, P. M. Lievens and S. H. Orkin, 1992 Human CCAAT displacement protein is homologous to the Drosophila homeoprotein, cut. Nat. Genet. **1:** 50–55.

Phillips, R. G., and J. R. Whittle, 1993 wingless expression mediates determination of peripheral nervous system elements in late stages of Drosophila wing disc development. Development **118:** 427–438.

Quaggin, S. E., G. B. Heuvel, K. Golden, R. Bodmer and P. Igarashi, 1996 Primary structure, neural-specific expression, and

chromosomal localization of Cux-2, a second murine homeobox gene related to Drosophila cut. J. Biol. Chem. **271:** 22624–22634.

Raisin, S., S. Pantalacci, J. P. Breittmayer and P. Leopold, 2003 A new genetic locus controlling growth and proliferation in *Drosophila melanogaster*. Genetics **164:** 1015–1025.

Richardson, H. E., L. V. O'Keefe, S. I. Reed and R. Saint, 1993 A Drosophila G1-specific cyclin E homolog exhibits different modes of expression during embryogenesis. Development **119:** 673–690.

Richardson, H., L. V. O'Keefe, T. Marty and R. Saint, 1995 Ectopic cyclin E expression induces premature entry into S phase and disrupts pattern formation in the Drosophila eye imaginal disc. Development **121:** 3371–3379.

Robertson, H. M., C. R. Preston, R. W. Phillis, D. M. Johnson-Schlitz, W. K. Benz *et al.*, 1988 A stable genomic source of *P* element transposase in *Drosophila melanogaster*. Genetics **118:** 461–470.

Rollins, R. A., P. Morcillo and D. Dorsett, 1999 Nipped-B, a Drosophila homologue of chromosomal adherins, participates in activation by remote enhancers in the *cut* and *Ultrabithorax* genes. Genetics **152:** 577–593.

Rollins, R. A., M. Korom, N. Aulner, A. Martens and D. Dorsett, 2004 Drosophila nipped-B protein supports sister chromatid cohesion and opposes the stromalin/Scc3 cohesion factor to facilitate long-range activation of the cut gene. Mol. Cell. Biol. **24:** 3100–3111.

Santaguida, M., Q. Ding, G. Berube, M. Truscott, P. Whyte *et al.*, 2001 Phosphorylation of the CCAAT displacement protein (CDP)/Cux transcription factor by cyclin A-Cdk1 modulates its DNA binding activity in G(2). J. Biol. Chem. **276:** 45780–45790.

Schneuwly, S., R. Klemenz and W. J. Gehring, 1987 Redesigning the body plan of Drosophila by ectopic expression of the homoeotic gene Antennapedia. Nature **325:** 816–818.

Sinclair, A. M., J. A. Lee, A. Goldstein, D. Xing, S. Liu *et al.*, 2001 Lymphoid apoptosis and myeloid hyperplasia in CCAAT displacement protein mutant mice. Blood **98:** 3658–3667.

Skalnik, D. G., E. C. Strauss and S. H. Orkin, 1991 CCAAT displacement protein as a repressor of the myelomonocytic-specific gp91-phox gene promoter. J. Biol. Chem. **266:** 16736–16744.

Sturtevant, M. A., M. Roark and E. Bier, 1993 The Drosophila rhomboid gene mediates the localized formation of wing veins and interacts genetically with components of the EGF-R signaling pathway. Genes Dev. **7:** 961–973.

Sudarsan, V., S. Anant, P. Guptan, K. Vijayraghavan and H. Skaer, 2001 Myoblast diversification and ectodermal signaling in Drosophila. Dev. Cell **1:** 829–839.

Toba, G., T. Ohsako, N. Miyata, T. Ohtsuka, K. H. Seong *et al.*, 1999 The gene search system: a method for efficient detection and rapid molecular identification of genes in *Drosophila melanogaster*. Genetics **151:** 725–737.

Truscott, M., L. Raynal, P. Premdas, B. Goulet, L. Leduy *et al.*, 2003 CDP/Cux stimulates transcription from the DNA polymerase alpha gene promoter. Mol. Cell. Biol. **23:** 3013–3028.

Valarche, I., J. P. Tissier-Seta, M. R. Hirsch, S. Martinez, C. Goridis *et al.*, 1993 The mouse homeodomain protein Phox2 regulates Ncam promoter activity in concert with Cux/CDP and is a putative determinant of neurotransmitter phenotype. Development **119:** 881–896.

van Wijnen, A. J., M. F. van Gurp, M. C. de Ridder, C. Tufarelli, T. J. Last *et al.*, 1996 CDP/cut is the DNA-binding subunit of histone gene transcription factor HiNF-D: a mechanism for gene regulation at the G1/S phase cell cycle transition point independent of transcription factor E2F. Proc. Natl. Acad. Sci. USA **93:** 11516–11521.

Verheyen, E. M., K. J. Purcell, M. E. Fortini and S. Artavanis-Tsakonas, 1996 Analysis of dominant enhancers and suppressors of activated Notch in Drosophila. Genetics **144:** 1127–1141.

Wakabayashi-Ito, N., M. P. Belvin, D. A. Bluestein and K. V. Anderson, 2001 fusilli, an essential gene with a maternal role in Drosophila embryonic dorsal-ventral patterning. Dev. Biol. **229:** 44–54.

Wang, Y., W. Zhang, Y. Jin, J. Johansen and K. M. Johansen, 2001 The JIL-1 tandem kinase mediates histone H3 phosphorylation and is required for maintenance of chromatin structure in Drosophila. Cell **105:** 433–443.

Wang, Z., A. Goldstein, R. T. Zong, D. Lin, E. J. Neufeld *et al.*, 1999 Cux/CDP homeoprotein is a component of NF-muNR and represses the immunoglobulin heavy chain intronic enhancer by antagonizing the bright transcription activator. Mol. Cell. Biol. **19:** 284–295.

Xu, Q., M. Li, J. Adams and H. N. Cai, 2004 Nuclear location of a chromatin insulator in Drosophila melanogaster. J. Cell Sci. **117:** 1025–1032.

Xu, T., and G. M. Rubin, 1993 Analysis of genetic mosaics in developing and adult Drosophila tissues. Development **117:** 1223–1237.

Zhang, W., Y. Wang, J. Long, J. Girton, J. Johansen *et al.*, 2003 A developmentally regulated splice variant from the complex lola locus encoding multiple different zinc finger domain proteins interacts with the chromosomal kinase JIL-1. J. Biol. Chem. **278:** 11696–11704.

Zimmer, C., M. C. Tiveron, R. Bodmer and H. Cremer, 2004 Dynamics of Cux2 expression suggests that an early pool of SVZ precursors is fated to become upper cortical layer neurons. Cereb. Cortex **14:** 1408–1420.

Communicating editor: J. Tamkun